2016

Mechanical Property Characterization of Polymeric Composites Reinforced by Continuous Microfibers

Ali Zubayar
South Dakota State University

MECHANICAL PROPERTY CHARACTERIZATION OF POLYMERIC COMPOSITES REINFORCED BY CONTINUOUS MICROFIBERS

BY

ALI ZUBAYAR

A thesis submitted in partial fulfillment of the requirements for the

Master of Science

Major in Mechanical Engineering

South Dakota State University

2016

MECHCANICAL PROPERTY CHARACTERIZATION OF POLYMERIC COMPOSITES REINFORCED BY CONTINUOUS MICROFIBERS

This thesis is approved as a creditable and independent investigation by a candidate for the Master of Science in Mechanical Engineering degree and is acceptable for meeting the thesis requirements for this degree. Acceptance of this does not imply that the conclusions reached by the candidate are necessarily the conclusions of the major department.

Zhong Hu, Ph.D.
Thesis Advisor Date

Kurt Bassett, Ph.D.
Head, Department of Mechanical Engineering Date

Dean, Graduate School Date

This thesis is dedicated to my only son.

ACKNOWLEDGEMENTS

1. This work was supported by funds from the South Dakota State Governor Research Center of ‘‘Composites and Nanocomposites Advanced Manufacturing (CNAM) Center”.
2. The Department of Mechanical Engineering at South Dakota State University.
3. The computational facility and technical support provided by Brian Moore, University High Performance Computing.
4. The College of Engineering at South Dakota State University.

CONTENTS

ABBREVIATIONS……vii

LIST OF FIGURES……viii

LIST OF TABLES……...xi

ABSTRACT……xiii

1. INTRODUCTION 1

1.1 Background 1

1.2 Fabrication Process 4

1.2.1 Filament Winding 4

1.2.2 Spray Molding 5

1.2.3 Pultrusion 6

1.2.4 Injection Molding 6

1.2.5 Prepreg 7

2. LITERATURE REVIEW 8

3. ISSUES AND MOTIVATION 13

3.1 Motivation 13

3.2 Issues 15

3.3 Objectives 16

3.4 Methodology 17

4. MODELING APPROACH 18

5. RESULTS 24

5.1 Case Study-1: 24

5.2 Case Study-2: 31

5.3 Case Study-3: 35

5.4 Case Study-4: 39

5.5 Case Study-5: 44

5.6 Case Study-6: 51

6. VALIDATION OF THE MODEL 55

6.1 First Order Model: 55

6.2 Second Order Model: 55

7. CONCLUSION 61
8. FUTURE WORKS 63
REFERENCES 64

ABBREVIATIONS

GPa	Giga Pascal
MPa	Mega Pascal
mm	millimeter
CNT	Carbon Nano Tube
ROM	Rule of Mixture
RVE	Representative Volume Element
FEA	Finite Element Analysis
3D	3 Dimensional
CF	Carbon Fiber
PEEK	Poly Ether Ether Ketone

LIST OF FIGURES

Figure 1: Conventional Fabric Composite Material. 3

Figure 2: Conventional Composite Material. 3

Figure 3: Schematic of Filament Winding [1] 5

Figure 4: Schematic of Spray Molding [2] 5

Figure 5 : Schematic of Pultrusion [3] 6

Figure 6 : Schematic of Injection Molding [4] 7

Figure 7: Schematic of Prepreg [5] 7

Figure 8: Schematic of different RVEs in two different continued micro-fiber arrangements in matrix. 15

Figure 9: Methodology 17

Figure 10: FEA Models for RVEs. 19

Figure 11: Uniaxial tensile loading in square-I, square-II, square-III, and hexagon-I, and hexagon-II. (Top and then left to right: front view and side views for square and hexagonal RVEs, respectively). 21

Figure 12: Lateral expansion loading in square-I, square-II, square-III, and hexagon-I, and hexagon-II. (Top and then left to right: front view and side views for square and hexagonal RVEs, respectively). 22

Figure 13: Transverse shear loading in square-I, square-II, square-III, hexagon-I, and hexagon-II. (Top and then left to right: front view and side views for square and hexagonal RVEs, respectively). 23

Figure 14: Expansion test for RVEs of IM7/PEEK material at carbon fiber volume percent of 54.7 vol%.(left: Axial Strain, 1st middle: Axial Stress, 2nd Middle: von Mises Strain and right: von Mises Stress) 25

Figure 15: Shear test for RVEs of IM7/PEEK material at carbon fiber volume percent of 54.7 vol%.(left: Axial Strain, 1st middle: Axial Stress, 2nd Middle: von Mises Strain and right: von Mises Stress) 26

Figure 16: Tensile test for RVEs of IM7/PEEK material at carbon fiber volume percent of 54.7 vol%.(left: Axial Strain, 1st middle: Axial Stress, 2nd Middle: von Mises Strain and right: von Mises Stress). 27

Figure 17: Material properties of the RVEs of IM7/PEEK extracted from modeling. (a) Young's moduli, Ex and Ez, and shear moduli, Gxy and Gzx, and (b) Poisson's ratios νxy, νyz, and νzx. 30

Figure 18: Material properties of the RVEs of Carbon Fiber/Epoxy extracted from modeling. (a) Young's moduli, Ex and Ez, and shear moduli, Gxy and Gzx, and (b) Poisson's ratios νxy, νyz, and νzx. 34

Figure 19: Material properties of the RVEs of Carbon Fiber/Polyamide 6 extracted from modeling. (a) Young's moduli, Ex and Ez, and shear moduli, Gxy and Gzx, and (b) Poisson's ratios νxy, νyz, and νzx. 38

Figure 20: Material properties of the RVEs of Glass Fiber/Epoxy extracted from modeling. (a) Young's moduli, Ex and Ez, and shear moduli, Gxy and Gzx, and (b) Poisson's ratios νxy, νyz, and νzx. 43

Figure 21: Finite Element Model of the 3-D orthogonal composite model. 45

Figure 22: Elastic properties of the 3D orthogonal fabric composites changing with carbon fiber volume fraction. (a) Shear moduli, (b) Young's moduli, and(c) Poisson's ratios. 48

Figure 23:Tensile test for 3D orthogonal fabric CF/Epoxy composites at carbon fiber volume percent of 52.65 vol %.(left: tensile in x-component, middle: tensile in y-component, and right: tensile in z-component 49

Figure 24: Shear test for 3D orthogonal fabric CF/Epoxy composites at carbon fiber volume percent of 52.65 vol %.(left: tensile in xy-component, middle: tensile in yz-component, and right: tensile in zx-component)..... 50

Figure 25: Finite Element Model of the 3-D laminate composite model. 52

Figure 26: Elastic properties of the 3D orthogonal fabric composites changing with carbon fiber volume fraction. (a) Shear moduli, (b) Young's moduli, and(c) Poisson's ratios. 54

Figure 27: Longitudinal young's modulus characteristics of Glass Fiber/Epoxy calculated from FEA modeling, theoretical rule of mixture model, and Experiment (20). 59

Figure 28: Transverse young's modulus characteristics of Glass Fiber/Epoxy composite materials calculated from FEA modeling, theoretical 1st order model, theoretical 2nd order model, and Experiment (19, 21)..... 59

Figure 29: In-plane shear modulus characteristics of Glass Fiber/Epoxy calculated from FEA modeling, theoretical 1st order model, theoretical 2nd order model, and Experiment (20)..... 60

LIST OF TABLES

Table 1: Material properties of carbon fiber and PEEK (z-axis: fiber direction). 24

Table 2: Material properties of the RVEs of IM7/PEEK extracted from modeling (z-axis: fiber direction). 28

Table 3: Comparison of material properties of the IM7/PEEK uni-directional carbon fiber composites (carbon fiber of 54.7 vol %) by modeling and experiments (z-axis: fiber direction). 31

Table 4: Material properties of carbon fiber and epoxy 31

Table 5 : Material properties of the RVEs of Carbon Fiber/Epoxy extracted from modeling (z-axis: fiber direction). 32

Table 6: Material properties of carbon fiber and Polyamide 6 (z-axis: fiber direction). 35

Table 7: Material properties of the RVEs of Carbon Fiber/Polyamide 6 extracted from modeling (z-axis: fiber direction). 36

Table 8: Material properties of glass fiber and Epoxy (z-axis: fiber direction). 39

Table 9: Material properties of the RVEs of Glass Fiber/Epoxy extracted from modeling (z-axis: fiber direction). 40

Table 10: Material properties of the 3D orthogonal fabric composites from modeling (In-plane of x-y, 7 layers in x-direction, 6 layers in y-direction, and thickness of z-direction). 46

Table 11: Comparison of material properties of the 3D orthogonal fabric case study composites (carbon fiber of 52.65 volume %) by modeling and experiments. 46

Table 12: Material properties of the 3D orthogonal composite laminate from modeling (In-plane of x-y, 7 layers in x-direction, 6 layers in y-direction, and thickness of z-direction). 52

Table 13: Comparison of material properties of the 3D laminate case study composites (carbon fiber of 52.65 volume %) by modeling, experiments, and predicted customized model. 53

Table 14: Mechanical Properties of glass fiber and epoxy and z is the fiber direction. 56

Table 15: Longitudinal young's modulus characteristics of Glass Fiber/Epoxy calculated from FEA modeling and theoretical model (z-axis: fiber direction). 56

Table 16: Transverse young's modulus characteristics of Glass Fiber/Epoxy calculated from FEA modeling and theoretical model (z-axis: fiber direction). 57

Table 17: In-plane Shear modulus characteristics of Glass Fiber/Epoxy calculated from FEA modeling and theoretical model (z-axis: fiber direction). 58

ABSTRACT

MECHANICAL PROPERTY CHARACTERIZATION OF POLYMERIC COMPOSITES REINFORCED BY CONTINUOUS MICROFIBERS

ALI ZUBAYAR

2016

Innumerable experimental works have been conducted to study the effect of polymerization on the potential properties of the composites. Experimental techniques are employed to understand the effects of various fibers, their volume fractions and matrix properties in polymer composites. However, these experiments require fabrication of various composites which are time consuming and cost prohibitive. Advances in computational micromechanics allow us to study the various polymer based composites by using finite element simulations. The mechanical properties of continuous fiber composite strands are directional. In traditional continuous fiber laminated composites, all fibers lie in the same plane. This provides very desirable increases in the in-plane mechanical properties, but little in the transverse mechanical properties. The effect of different fiber/matrix combinations with various orientations is also available. Overall mechanical properties of different micro continuous fiber reinforced composites with orthogonal geometry are still unavailable in the contemporary research field.

In this research, the mechanical properties of advanced polymeric composite reinforced by continuous micro fiber will be characterized based on analytical investigation and FE computational modeling. Initially, we have chosen IM7/PEEK, Carbon Fiber/Nylon 6, and Carbon Fiber/Epoxy as three different case study materials for analysis. To obtain the equivalent properties of the micro-hetero structures, a concept of micro-scale

representative volume elements (RVEs) is introduced. Five types of micro scale RVEs (3 square and 2 hexagonal) containing a continuous micro fiber in the polymer matrix were designed. Uniaxial tensile, lateral expansion and transverse shear tests on each RVE were designed and conducted by the finite element computer modeling software ANSYS. The formulae based on elasticity theory were derived for extracting the equivalent mechanical properties (Young's moduli, shear moduli, and Poisson's ratios) from the numerical solutions of the RVEs undergone these three load tests. Validation of the obtained micro-scale mechanical properties will be performed using rule of mixture (ROM), 1st, and 2nd order of the mathematical model and experimental data.

1. INTRODUCTION

1.1 Background

The necessity of composite materials is increasing in every aspects of our life. The unending desire for getting lighter, stronger and cheaper materials is the key behind this increased use. Composite materials are stuffing recess in the automotive industry by yielding lightweight, strong substitute to steels and aluminums in an attempt to intensify fuel efficiency. Moreover, these materials can increase the longevity of automobiles due to the highly corrosion resistant feature. In military applications ranging from lightweight weaponry and body armor to shipboard superstructure applications are made by composites. Also the aerospace manufacturer industry and research organizations use composites not only because of its strength to weight ratio but also for its thermal and mechanical properties in the extreme environments. The “Shielding tiles” used to protect the space shuttle upon atmospheric reentry is an example of the composite materials. Composite materials are also used in the vicious environment of the human body by the medical community. Due to increased resistance to high temperature creep property, composites are still used as a turbine blade.

Composite materials can be defined as,

- Two or more chemically distinct materials.
- Have improved properties over the individual materials.
- Can be produced by various processing techniques.
- Provide desired structural, electrical, mechanical, and thermal properties.
- Could be natural or synthetic. [1]

The basic feature of the fiber, variety of matrix, the interface properties, the building and geometry of the materials are determining characteristics of the composite materials. They are dominant over traditional materials like metals and ceramics due to having high specific modulus, high specific strength, high resistance to corrosion, light weight and tailoring compatibility to meet the specific purpose.

The most important criteria of any composite material are depend on the characteristics of its reinforcement materials, known as fiber. Fiber is the core material which comply the desired conditions and transfer strength to the matrix component effecting and intensifying their properties as required. Due to several factors fibers are falling in ideal performance of a composite material. The performance of a fiber composite is justified by its length, shape, and composition of the fibers, orientation and the mechanical properties of the matrix materials. The fiber orientation inside the matrix is the indicator of the strength of the composite materials. Along the longitudinal direction of the fiber, this strength is getting higher. This doesn't imply that the longitudinal fiber can sustain the equal amount of load irrespective of the applied direction. But the observed performance of the longitudinal fiber can be optimum when the load is applied along its direction. On the other hand, the strength of the composite will be drastically reduced if the applied load makes slightest shift in the angle of loading. Therefore, unidirectional loading is found in few structures and hence it is advisable to give a mix of orientations for fibers in composites particularly for the applied load will be significantly heavier.

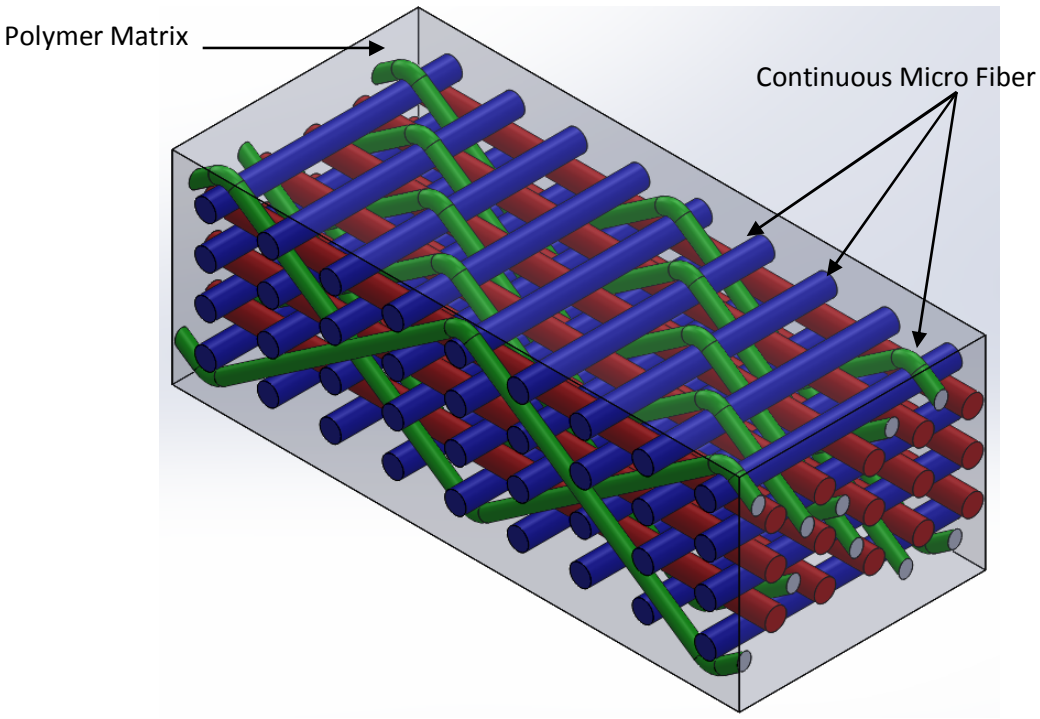

Figure 1: Conventional Fabric Composite Material.

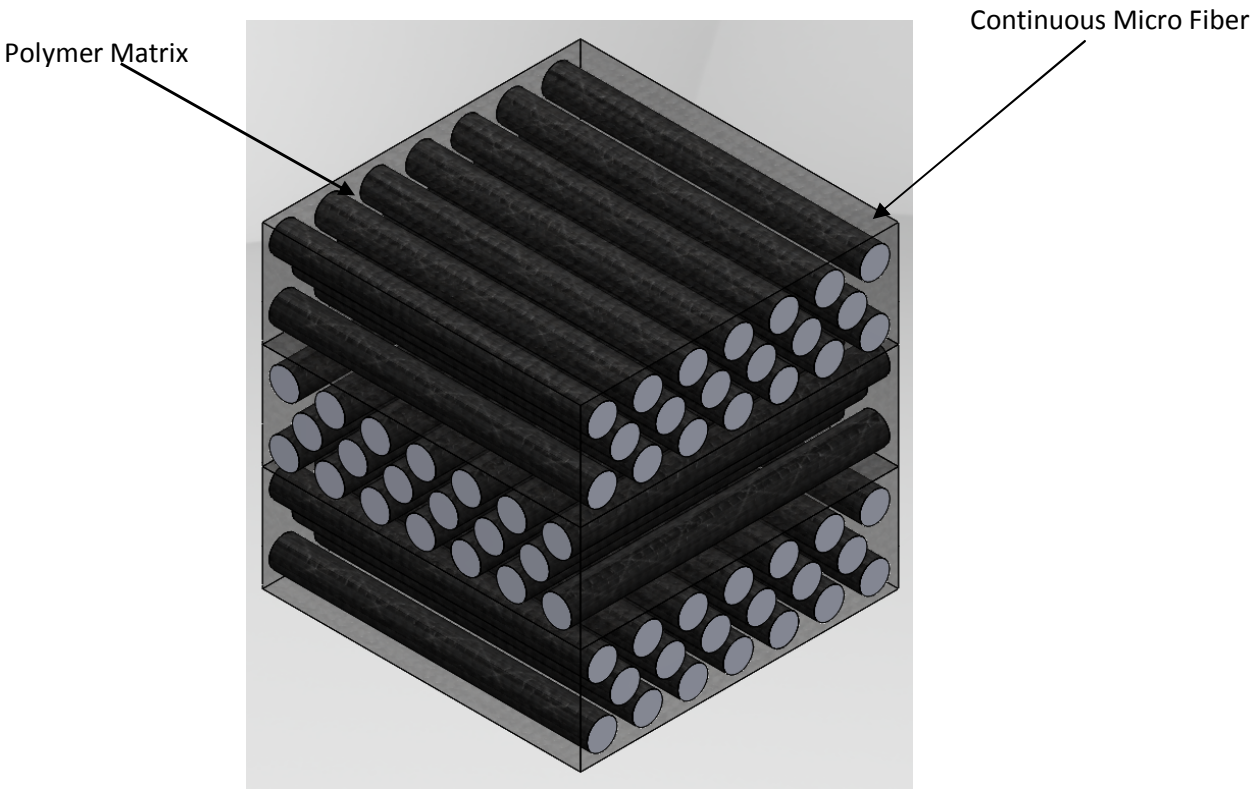

Figure 2: Conventional Composite Material.

In comparison with standard fiber reinforced polymer (FRP) matrix composites, polymer matrix composites are more advanced materials. Polymer matrix composite can have,

I. High strength to weight ratio
II. High stiffness to weight ratio
III. High fatigue resistance
IV. No catastrophic failure
V. Low thermal expansion in fiber oriented directions
VI. Resistance to chemicals and environmental factors

Polymer matrix composites also have stronger pliability as compared to other ordinary reinforced composites. In general, it contains a high modulus fiber with low modulus matrix. The stiffness and load bearing qualities can be achieved by the fiber with high modulus, whereas the low-modulus fiber makes the composite more damage tolerant and keeps the material cost low. By changing fractional fiber volume ratio (%) and stacking sequence of different plies the mechanical properties of a polymer matrix composite material can be varied. Besides, due to balanced effective properties, reduced weight and/or cost, with improvement in fatigue and impact properties are the specific advantages of polymer matrix composites over conventional composites. [2]

1.2 Fabrication Process

1.2.1 Filament Winding

- The filament (or tape, tow, or band) is either precoated with the polymer or is drawn through a polymer bath so that it picks up polymer on its way to the winder.
- Productivity is high (50 kg/h).

- Fabrication of composite pipes, tanks, and pressure vessels. Carbon fiber reinforced rocket motor cases used for Space Shuttle and other rockets are made this way.[2]

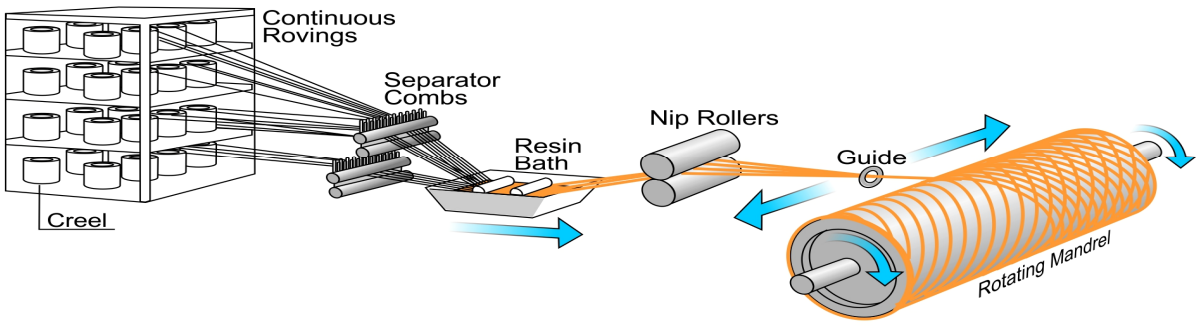

Figure 3: Schematic of Filament Winding [1]

1.2.2 Spray Molding

- A spray gun supplying resin in two converging streams into which roving is chopped
- Automation with robots results in highly reproducible production.
- Labor costs are lower.[2]

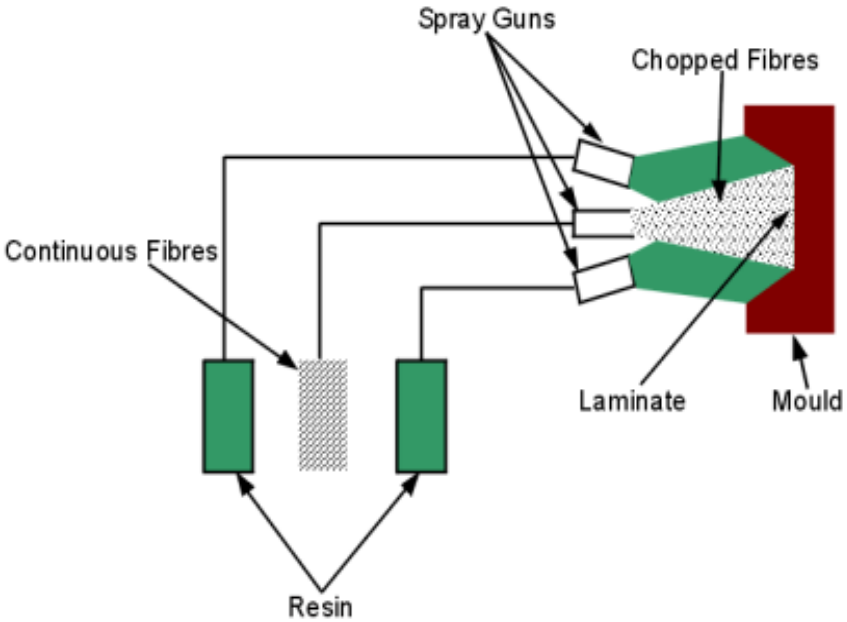

Figure 4: Schematic of Spray Molding [2]

1.2.3 Pultrusion

- Continuous fibers pulled through resin tank, then performing die and oven to cure.
- Production rates around 1 m/min.
- Applications are to sporting goods (golf club shafts), vehicle drive shafts (because of the high damping capacity), nonconductive ladder rails for electrical service, and structural members for vehicle and aerospace applications.[2]

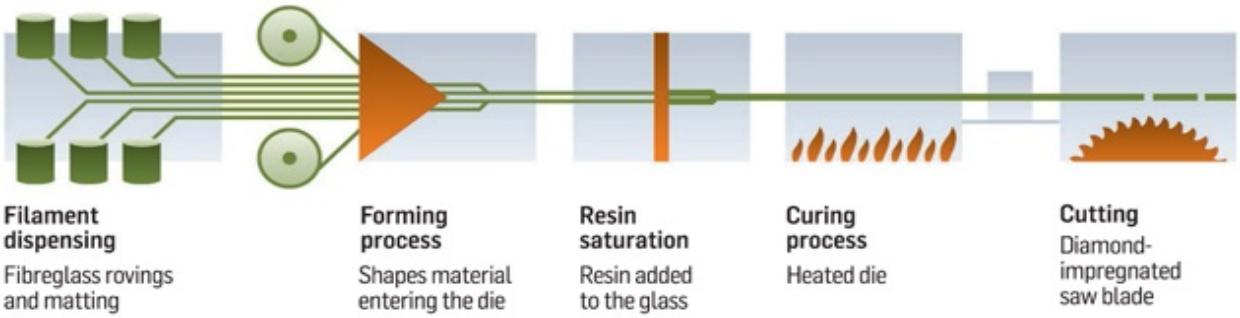

Figure 5 : Schematic of Pultrusion [3]

1.2.4 Injection Molding

- Process uses two resin components which are combined and mixed together, then injected into a mold cavity containing reinforcement.
- In the mold cavity, the resin rapidly reacts and cures to form the composite part.
- Automotive bumpers, fender and panel components, appliance housings, and furniture components.[2]

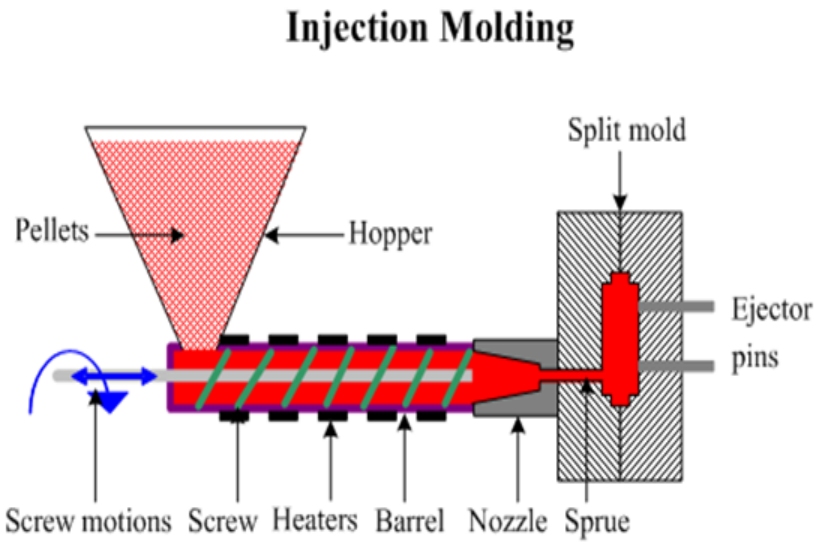

Figure 6 : Schematic of Injection Molding [4]

1.2.5 Prepreg

- Fabrics and fibers are pre-impregnated under heat and pressure or with solvent, or a pre-catalysed resin.
- Resin/catalyst levels and the resin content in the fiber are accurately set by the materials manufacturer.
- High fiber contents can be safely achieved.[2]

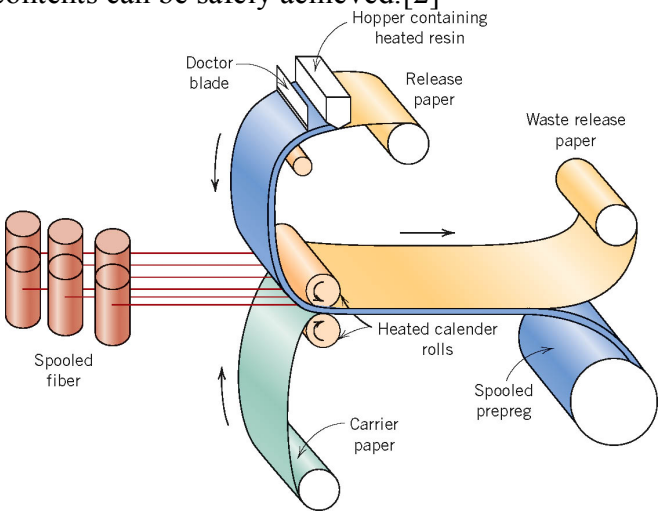

Figure 7: Schematic of Prepreg [5]

2. LITERATURE REVIEW

Recently, researchers have paid additional consideration to a process combining hybrid perform and squeeze casting to fabricate composites reinforced with different types of reinforcements, in which both particles and short fibers are employed .Since hybrid composites are produced by adding two reinforcements into matrix materials, their outstanding properties can be obtained by mixing the advantages of different sizes of short fibers, and particles, which yield a high degree of design freedom. They provide large opportunities to optimize the engineering performance of metal matrix composites for potential applications in the automotive industry, where relatively low volume of reinforcement is required.

Z. Hu *et al*. [8] proposed a two steps modeling approach has effectively predicted the mechanical properties of 3D carbon fiber-reinforced epoxy composites. A 13 layer 3D orthogonal fabric composite with binding of warp yarns through the thickness and carbon fiber of 52.65% volume was selected as the case study material. The modeling results show that the Young's moduli in fiber oriented directions and shear moduli are significantly higher than that of the matrix.

Sayan Banarjee *et al*. [9] conducted a research to study the representative volume element of a unidirectional hybrid composite using finite element method. The fibers were assumed to be circular and packed in a hexagonal array. The effects of volume fractions of the two different fibers used and also their relative locations within the unit cell are studied. Modified Halpin–Tsai equations were proposed for predicting the transverse and shear moduli of hybrid composites. Analytical results are obtained for all the elastic constants. The results for hybrid composites were compared with single fiber composites.

Bai-Chen Wang *et al.* [10] at their work, tried to improve the properties of the polymer using carbon nanotubes. They used carboxylic acid functionalized CNTs to develop a nano composite matrix for hybrid multi scale composites combining benefits of nanoscale reinforcement with well-established fibrous composites. CNTs were dispersed in epoxy by using high energy sonication. At low contents of CNTs, hybrid multi scale composites specimens were manufactured via resin transfer molding (RTM) process. It was also demonstrated that the addition of small amount of CNTs (0.025 wt. %) to epoxy for the fabrication of multi scale carbon fabric composites via RTM route effectively improves the matrix-dominated properties of polymer based composites.

A.Y. Boroujeni *et al.* [11] conducted a research to study the in-plane and out-of plane properties of fiber reinforced polymer composites (FRPs) by growing carbon nanotubes (CNTs) on carbon fibers. A relatively low temperature synthesis technique was utilized to directly grow CNTs over the carbon fibers. The on-axis tensile strength and ductility of the hybrid FRPs were improved by 11% and 35%, respectively, due to the presence of the thermal barrier coating (TBC) and the surface grown CNTs. This configuration also exhibited 16% improvement on the off-axis stiffness. Results from the experiment suggested that certain CNT growth patterns and lengths are more pertinent than the other surface treatments to achieve superior mechanical properties.

Yongli Zhang *et al.* [12] investigated the hybrid effects of the composites by studying the mechanical behaviors of unidirectional flax and glass fiber reinforced hybrid composites. A modified model for calculating the tensile strength was given based on the hybrid effect of tensile failure strain. The tensile properties of the hybrid composites were

improved with the increasing of glass fiber content. The macro-scale results had been correlated with the twist flax yarn structure, rough surface of flax fiber and fiber bridging between flax fiber layers and glass fiber layers.

Doo Jin Lee *et al.* [13] analyzed effective elastic modulus for multi phased hybrid composites. They introduced the characteristics of fiber length distribution (FLD) and fiber orientation distribution (FOD) of short fiber reinforced composites to determine mechanical properties of the composites. Interaction between the particles and matrix was considered by using a perturbed stress–strain theory, the Tandon–Weng model. In addition, the laminating analogy approach (LAA) was used to predict the overall elastic modulus of the composite. The theoretical and experimental platform was expected to provide more insightful understanding on any kinds of multiphase hybrid composites.

Shao-Yun Fu *et al.* [14] also investigated the elastic modulus of hybrid particle/short-fiber/polymer composites using the rule of hybrid mixtures (RoHM) equation and the laminate analogy approach (LAA). The elastic modulus of the hybrid composite was evaluated from the two single system, particle/polymer system and short-fiber/polymer system using the RoHM. The modulus of the short-fiber reinforced effective-matrix composite was estimated using LAA. The analysis suggested that the modulus of hybrid particle/short-fiber/polymer composites showed a positive hybrid effect.

N. Venkateshwaran *et al.* [15] also predicted the tensile strength and modulus of short, randomly oriented hybrid-natural fiber composite using Rule of Hybrid Mixture (RoHM). Hybrid composites were prepared using banana/sisal fibers of 40:0, 30:10, 20:20, 10:30, and 0:40 ratios, while overall fiber volume fraction was fixed as 0.4Vf. The comparison between experimental and RoHM showed that they were in good agreement.

T. George *et al.* [16] developed Carbon fiber reinforced polymer (CFRP) composite sandwich panels with hybrid foam filled CFRP pyramidal lattice core. Those lattice cores had been assembled from linear carbon fiber braids and Divinycell H250 polymer foam trapezoids. Those had been stitched to 3D woven carbon fiber face sheets and infused with an epoxy resin using a vacuum assisted resin transfer molding process. Sandwich panels with carbon fiber composite truss volumes of 1.5–17.5% of the core volume had been fabricated. The through thickness modulus and strength of the hybrid cores was found to increase with increasing truss core volume fraction.

Leon Mishnaevsky Jr. *et al.* [17] conducted a research on the strength and damage resistance of hybrid and hierarchical composites through computational micromechanical models. It was shown that while glass/carbon fibers hybrid composites clearly demonstrate higher stiffness and lower weight with increasing the carbon content, they can have lower strength as compared with usual glass fiber polymer composites.

R. Muñoz *et al.* [18] studied on the deformation and failure micro mechanisms of a hybrid 3D woven composite under tensile load. Plain and open-hole composite coupons were tested in tension until failure in the fill and warp directions, as well as fiber tows extracted from the dry fabric and impregnated with the matrix. The experimental observations and the predictions of an isostrain model were used to understand the key factors controlling the elastic modulus, strength and notch sensitivity of hybrid 3D woven composites in tension. It was found that the full contribution of the glass fibers to the composite strength was not employed, due to the premature fracture of the carbon fibers, but their presence increased the fracture strain and the energy dissipated during fracture.

S. Rahmanian *et al.* [19] fabricated a high performance multi scale composite by incorporating carbon nanotubes (CNT) and short carbon fibers into an epoxy matrix. . To improve the stress transfer between epoxy and carbon fibers, CNT were also grown on fibers through chemical vapor deposition (CVD) method to produce CNT grown short carbon fibers (CSCF). The multi scale composites revealed significant improvement in elastic and storage modulus, strength as well as impact resistance in comparison to CNT–epoxy or CSCF–epoxy composites. An optimum content of CNT was found which provided the maximum stiffness and strength.

After reviewing the existing literature available on hybrid multi scale fiber composites, particularly carbon fiber composites put effort to understand the basic needs of the growing composite industry. The conclusions drawn from this is that, the success of combining carbon fibers with polymer matrices results in the improvement of mechanical properties of the composites compared with other fiber reinforced matrix materials.

3. ISSUES AND MOTIVATION

3.1 Motivation

Composites provide engineers the distinctive capability to tailor material properties to particular applications. By integrating two or more constituent materials, a resultant can be fabricated with varying mechanical and thermal properties. This resultant is not a solution, but two or more separate material as the constituents hold their individual identities in the composites. The constituents' minimized specific weight to strength ratios, increased or decreased stiffness, targeted coefficients of thermal expansion, and increased toughness are but a few of the advantages to composites. Often the advantages are manifested in cost savings due to lighter materials, increased fatigue life, and increased reliability.

Due to attractive physical, mechanical and thermal properties and great potential for tailoring the properties through design Composite materials have a flexible field of applications. Micro fibers reinforcement in the polymeric composites will be one of the propitious developments in the arena of composites designs.

To anticipate the desired mechanical properties of hybrid short fiber composites i.e. strength and modulus, rule of mixtures (RoHM) equation is widely used. However, it is proved that RoHM performs better for longitudinal modulus of the polymer matrix composites. Though the overall stiffness for a given fiber volume fraction is not affected much by the variability in fiber location until elastic constants of a composite are volume averaged over the constituent micro phases. On the other hand, the strength values are very much dependent on the fiber/matrix interaction and interface quality parallel with the function of strength of the constituents. While in tensile test on the specimen, any

minor (microscopic) imperfection may lead to stress build-up and failure which could not be predicted directly by RoHM equations.[8]

The difficulty in modeling the behavior of polymeric composite materials makes it challenging to develop approaches that can lead to “Materials by Design”. Additionally, a number of advanced composites have hierarchical microstructures that span from nano to macro-scale, which require notable advancement of the present modeling and simulation methods.[2]

From the invention of carbon nanotube (CNT) by Lijima, the properties of the composites materials incorporated with CNT and carbon nano fiber become significantly influenced. The transversely isotropic property of continuous carbon fibers blended with CNT reinforced matrix expected to have desirable strength and stiffness compare with other conventional fiber matrix combinations. In this research, a 3-D orthogonal fabric composite will be generated. Based on the initial evaluated properties of the representative volume elements (RVE’s) of various micro fiber reinforced with polymer matrix will be developed.[8]

A concept of micro-scale representative volume elements (RVEs) is one of the effective tools to determine the properties of composite materials. RVE refers to a sample of the material that structurally has the entire characteristics of the mixture on the average, typically represented by a square, hexagonal prismatic bar or parallelogram containing one or more fiber. Five types of micro scale RVEs (3 square and 2 hexagonal) containing a continuous micro fiber in the polymer matrix can be designed to predict the properties of individual RVE.

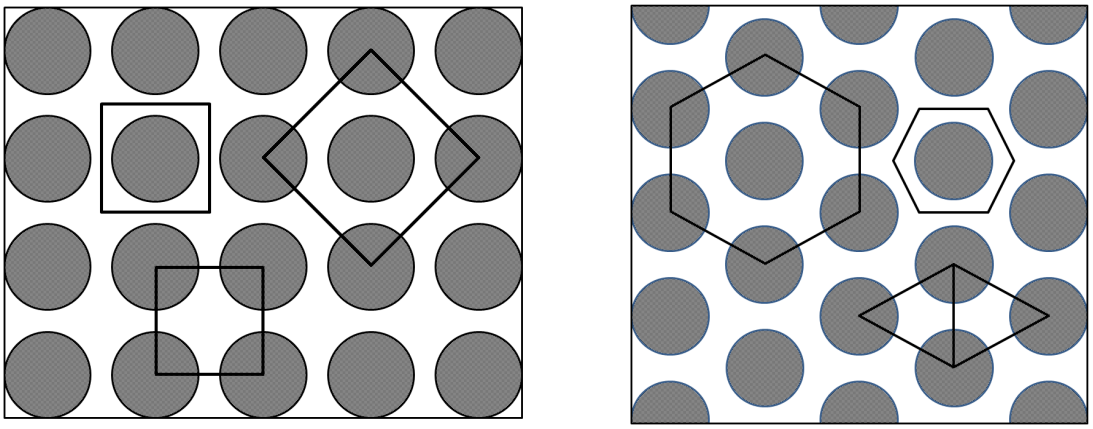

Figure 8: Schematic of different RVEs in two different continued micro-fiber arrangements in matrix.

Computational models are very effective in developing approaches that can predict the materials properties across length scales. Such methodologies are gaining more significance due to the recent surge in the use of composites in structural applications. After evaluating the properties of the initial fiber reinforced composite, two 3D orthogonal models of the micro fiber reinforced matrix will be used to predict overall Young's modulii, Shear modulii, and Poisson's ratios for a specified unit cell.

3.2 Issues

Polymer matrix composites have been studied for more than 30 years. To study the effect of polymerization on the potential properties of the composite innumerable experimental works have been conducted. Experimental techniques can be employed to understand the effects of various fibers, their volume fractions and matrix properties in polymer matrix composites. However, these experiments require fabrication of various composites which are time consuming and cost prohibitive. Advances in computational micromechanics allow us to study the various hybrid systems by using finite element simulations.

On the other hand, the mechanical properties of continuous fiber composite strands are directional. In traditional continuous fiber laminated composites, all fibers lie in the same plane. This provides very desirable increases in the in-plane mechanical properties, but little in the transverse mechanical properties.

Extensive research works being conducted on polymer composite materials by considering various assumptions. Some of them were focused on the orthogonal fabric composites. The effect of different fiber/matrix combinations with various orientations is also available. Overall mechanical properties of different micro fiber reinforced polymer matrix composites with orthogonal geometry are still unavailable in the contemporary research field.

In order to evaluate the potential of different ways of the material optimization and to develop recommendations for the production of new, strong and reliable composites, computational studies of the various microstructures of materials and their behavior under service conditions are required.

3.3 Objectives

The objective of this research is to understand and predict the mechanical properties of micro fiber reinforced composites based on analytical investigation and computational modeling. To mathematically evaluate/predict the performance of a polymeric composite reinforced by micro fibers, three steps (objectives) need to be followed (realized):

Step 1/Objective 1: Evaluate/Predict the performance of a unidirectional fiber reinforced composite with different polymer matrices

Step 2/Objective 2: Evaluate/Predict the performance of a 3-D orthogonal polymeric matrix composite reinforced by continuous micro fibers;

Step 3/Objective 3: Evaluate/Predict the performance of a 3-D laminated polymeric composite reinforced by continuous micro fibers.

3.4 Methodology

The overall thesis analysis will be performed as per the following flow chart:

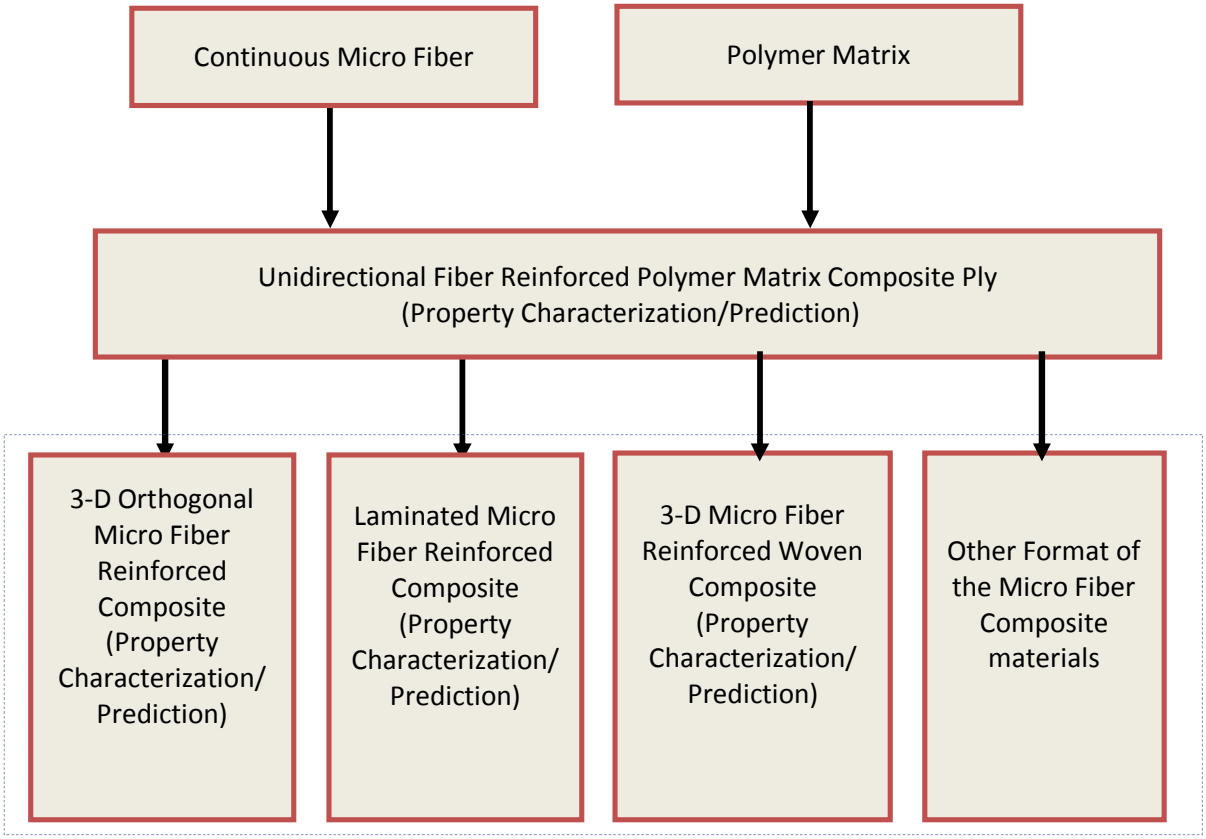

Figure 9: Methodology

4. MODELING APPROACH

Step 1: Characterize/Predict the performance of a polymeric matrix composite reinforced by microfibers

Based on various applications, different types of composite materials provides different role. The mechanical properties of each composite material depend upon their fiber matrix orientations, binder properties and geometrical shape. Also, depending on types of fiber and matrix materials and their property the overall performance varies significantly. Research outcome on various composite materials on microlevel therefore provides the best solution for so many critical applications such as space craft, high temperature equipment, medical devices etc.

In this research, we are basically focused on various types of polymer matrix composite reinforced by continuous micro fibers. Initially, we have chosen IM7/PEEK, Carbon Fiber/Nylon 6, and Carbon Fiber/Epoxy as three different case study materials for analysis. The mechanical behavior of 3D fabric composites has been characterized through analytical and numerical methods at the unit cell level, or representative volume element levels.

At the primary stage, a micro-scale representative volume elements concept is introduced to obtain the equivalent mechanical properties of the micro-hetero structures. RVE is the sample material that is structurally identical to the whole characteristics of the mixture on an average, typically presented as square, hexagonal prismatic bar or parallelogram contains one or several number of fibers. In this analysis basically five types of micro scale micro scale RVEs (3 square and 2 hexagonal) containing a continuous micro fiber in the polymer matrix were considered. Using finite element computational modeling software ANSYS education version uniaxial tensile, lateral expansion and transverse shear tests on each RVE were designed and conducted. From the numerical solutions of the five RVEs undergone through the three loading condition the formulae based on elasticity theory were derived for extracting the equivalent mechanical

properties (Young's moduli, shear moduli, and Poisson's ratios) . In the secondary step, a finite element analysis (FEA) model for each RVE is generated to characterize the effective mechanical properties, as shown in Fig.9, to evaluate the mechanical properties of the polymeric matrix composite reinforced by continued microfibers.[8]

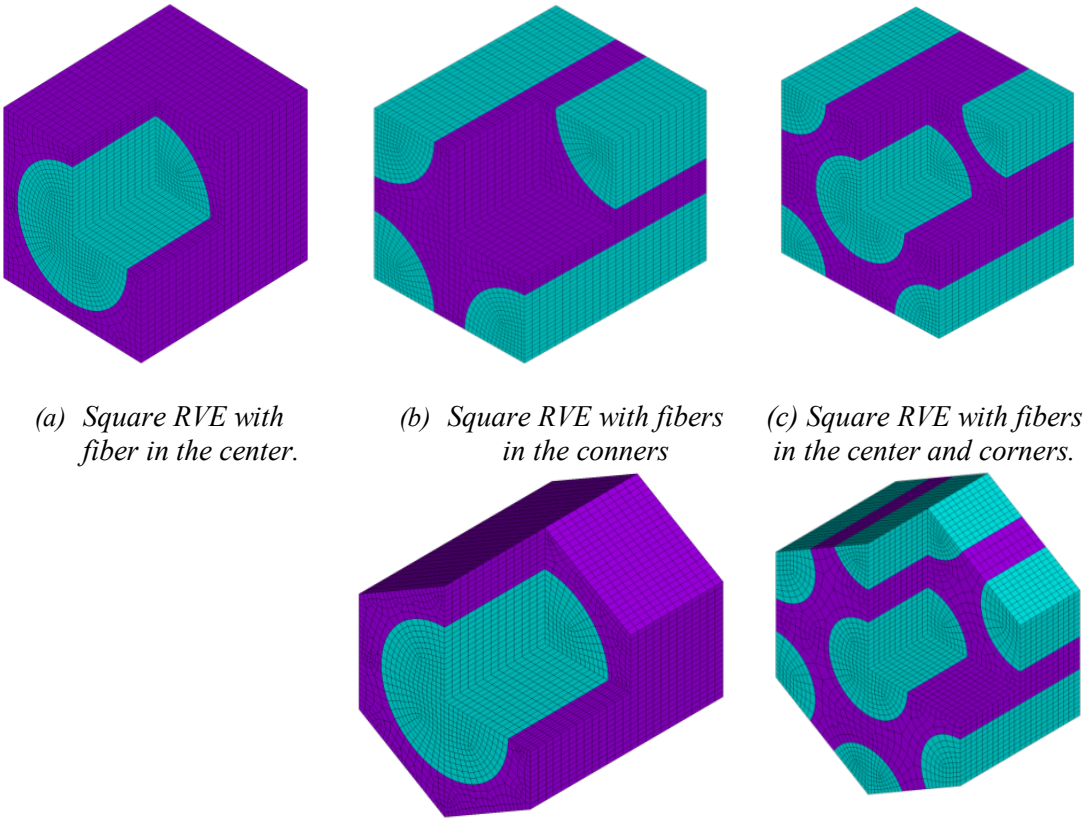

(a) Square RVE with fiber in the center.

(b) Square RVE with fibers in the conners

(c) Square RVE with fibers in the center and corners.

(d) Hexagon RVE with fiber in the center

(e) Hexagon RVE with fibers in the center and corners

Figure 10: FEA Models for RVEs.

Equations Used For predicting Mechanical Properties of RVE's:

To extract the equivalent material constants i.e. Young's Moduli E and Poisson's constants v the three load cases are applied to the square and hexagonal. At first, all five different RVEs are undergone a uniaxial tension ΔL, resulting in an average lateral contraction of Δa (Δa<0) for each side, as shown in Fig. 10. The Young's modulus, Ez, can be calculated by,

$$E_z = \sigma_z/\epsilon_z = (L/\Delta L)\sigma_z$$

And the Poisson's ratio, vzx, is, $v_{zx} = -(\Delta a/a)/(\Delta L/L)$

Then, the RVEs are undergone a lateral expansion by applying a lateral negative pressure p. Here, in the z-direction at both ends are constrained so that the plane strain condition is maintained, resulting in an expansion of average equivalent Δx in x-direction, as shown in Fig.11. Since the RVEs are under the hydrostatic pressure of -p, hence, providing, $\sigma_x = \sigma_y = p$ the following relationship can be derived as, $\frac{\Delta x}{pa} = -\left(\frac{v_{xy}}{E_x} + \frac{v^2{}_{zx}}{E_z}\right) + (\frac{1}{E_x} - \frac{v^2{}_{zx}}{E_z})$

According to the rule of mixture based on the volume percentages of the carbon fiber and the matrix in the RVEs vxy can be estimated. Therefore, the equivalent Young's modulus, Ex, can be determined as, $E_x = E_y = (1 - v_{xy})/(2v^2{}_{zx}/E_z + \Delta x/pa)$

Finally, under the transverse shear, as shown in Fig.12, similar to the cylindrical RVE, the equivalent shear modulus, Gzy, can be calculated as,

$$G_{zy} = G_{zx} = \tau_{zy}/\gamma_{zy} = F_s/A\gamma_{zy}$$

Where cross sectional area $A = 4a^2$ for the square RVE and $A = 6a^2/\sqrt{3}$ for the hexagonal RVE [8].

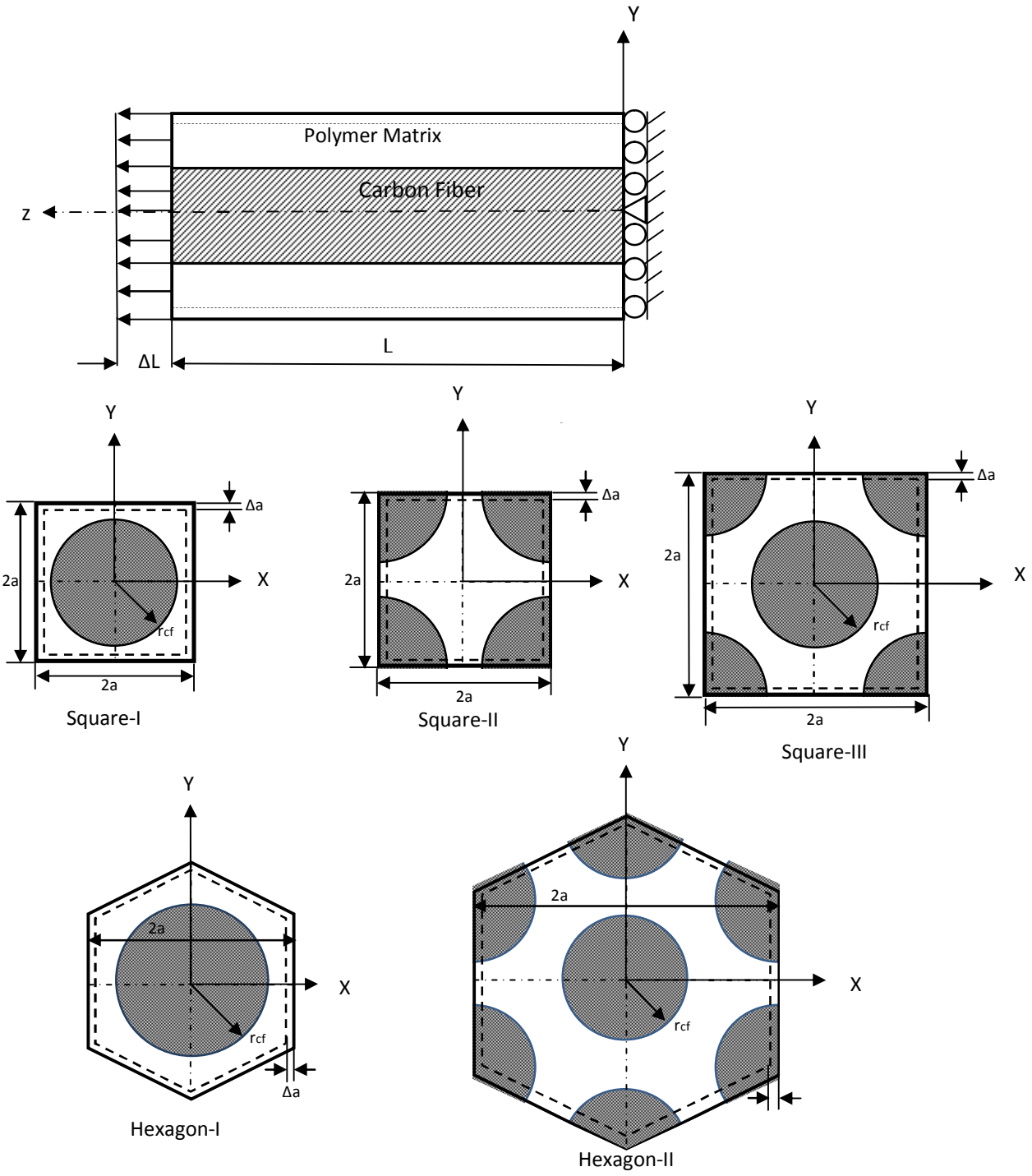

Figure 11: Uniaxial tensile loading in square-I, square-II, square-III, and hexagon-I, and hexagon-II. (Top and then left to right: front view and side views for square and hexagonal RVEs, respectively[8]).

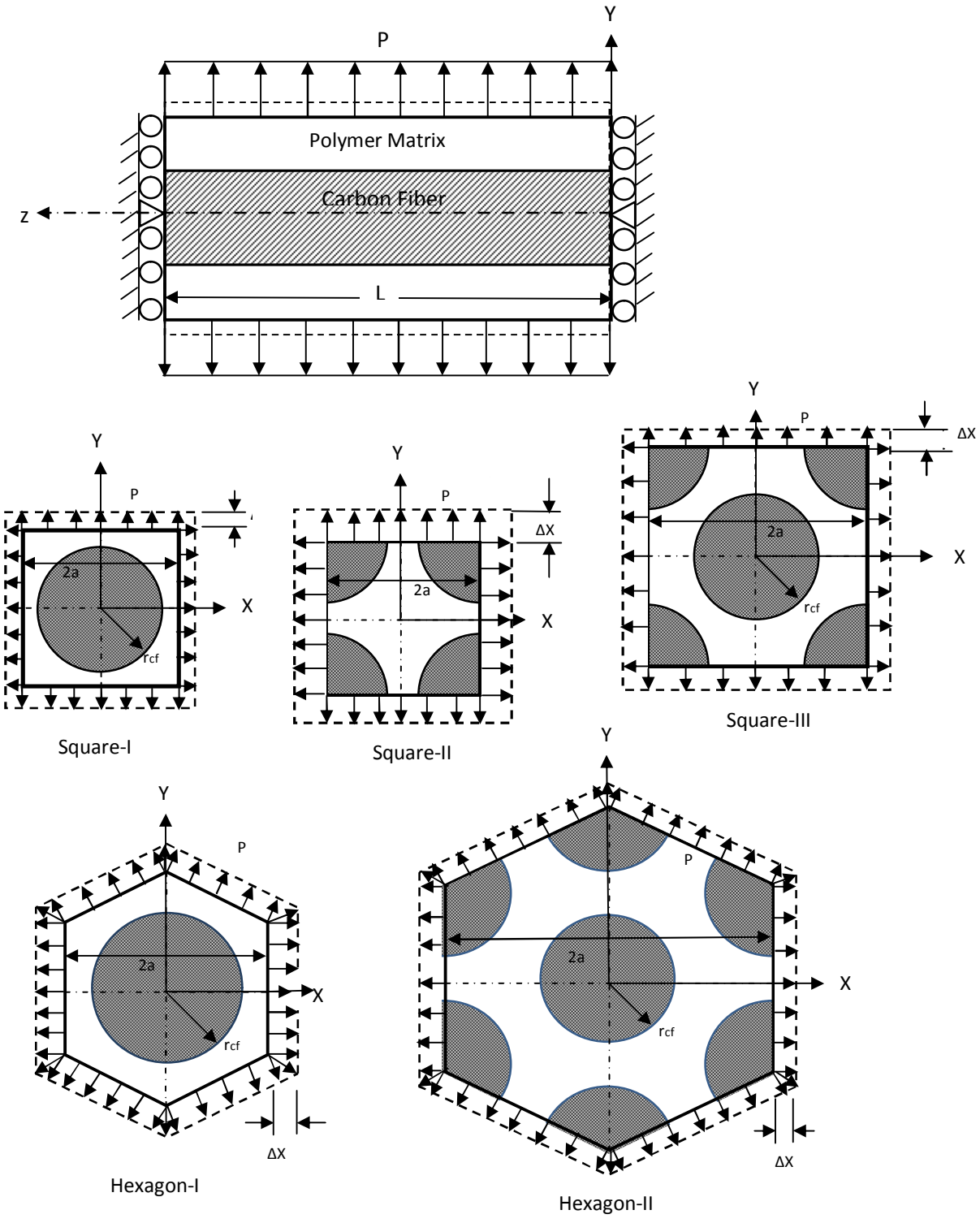

Figure 12: Lateral expansion loading in square-I, square-II, square-III, and hexagon-I, and hexagon-II. (Top and then left to right: front view and side views for square and hexagonal RVEs, respectively[8]).

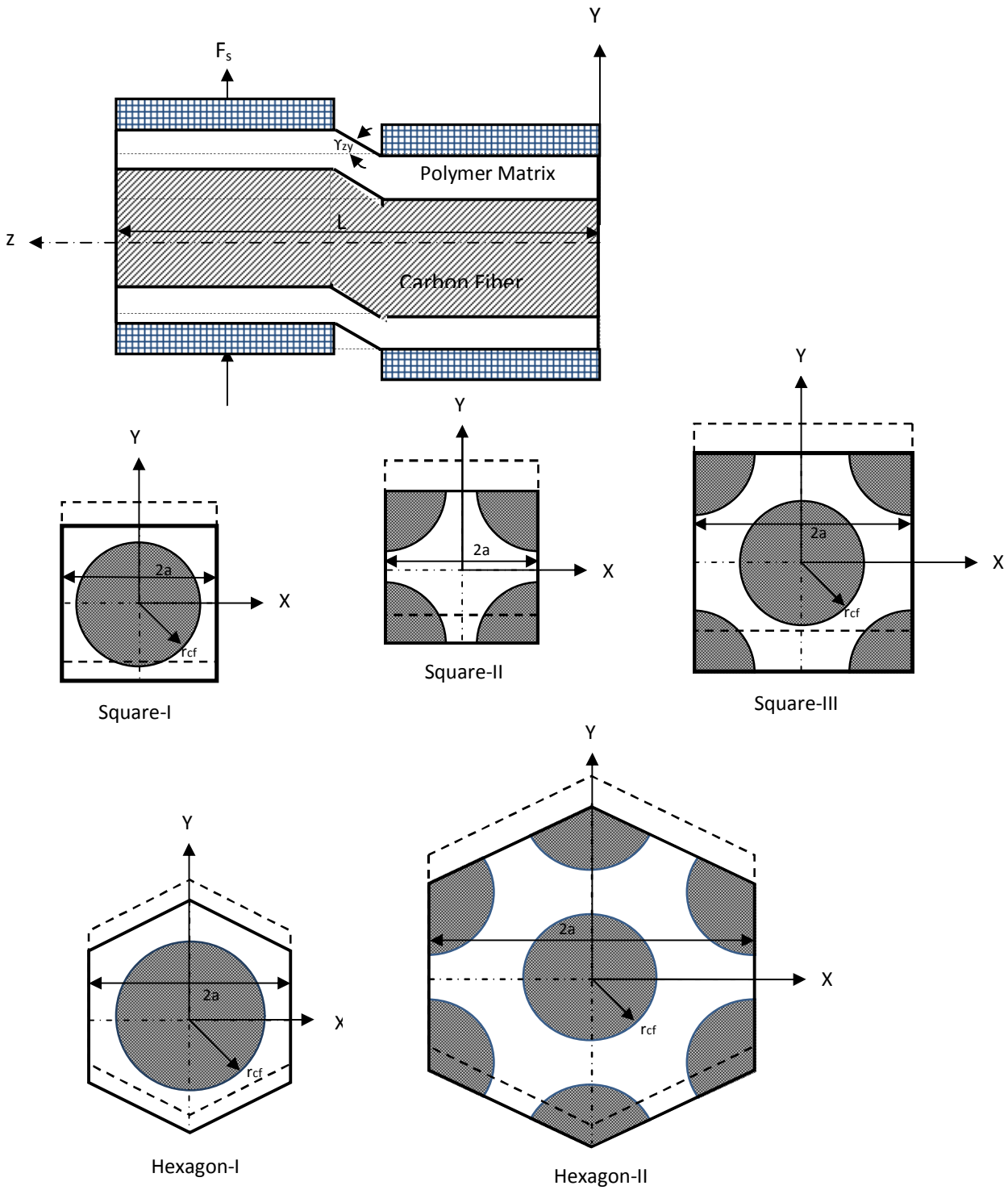

Figure 13: Transverse shear loading in square-I, square-II, square-III, hexagon-I, and hexagon-II. (Top and then left to right: front view and side views for square and hexagonal RVEs, respectively[8]).

5. RESULTS

5.1 Case Study-1:

For measuring the carbon fiber diameters and volume fraction, the samples were cut from the composite plate by water jet machine and molded and polished, and then Keyence VHX-600 Digital Microscope were used for measurements. The average fiber diameter was found to be 5.2µm and the fiber volume percentage is 54.7%. The material elastic properties of carbon fibers and polyether-ether-ketone (PEEK) are listed in the following Table 1.

Table 1: Material properties of carbon fiber and PEEK (z-axis: fiber direction).

Material	$E_x=E_y$ (GPa)	E_z (GPa)	$\nu_{xy}=\nu_{yx}$	$\nu_{zx}=\nu_{zy}$	$\nu_{xz}=\nu_{yz}$	G_{xy} (GPa)	G_{zx} (GPa)
Carbon Fiber	22.4	250	0.35	0.30	0.027	8.30	22.1
PEEK	3.60	3.60	0.36	0.36	0.36	1.32	1.32

To evaluate the effective mechanical properties of the IM7/PEEK uni-directional carbon fiber reinforced composites, the square and hexagonal RVEs with a continuous carbon fiber in the matrix in each RVE is studies. PEEK is considered as the matrix material. The deformation and stresses are modeled and computed for the three test cases to extract the equivalent material constants for the RVEs using afore described equations. The commercial FEA software ANSYS® was used for modeling. The FEA models for different RVEs are shown in Fig.9. Eight-node 3D solid structure elements of SOLID185 are employed. The proper element size and element density distribution, total elements, and total nodes are determined through convergence study of the extracted material properties and stress-strain distributions so that the modeling results are mesh-independent.

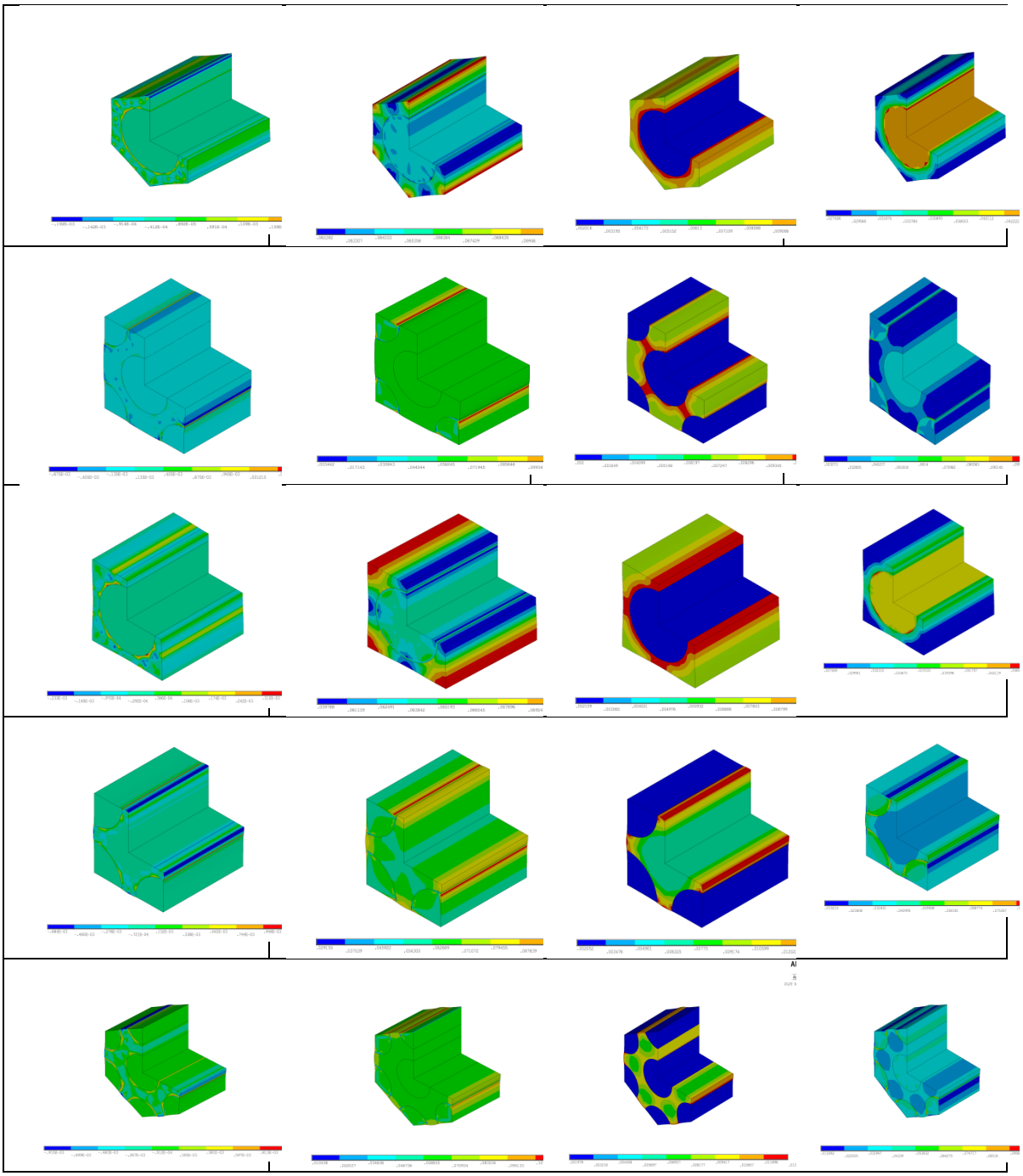

Figure 14: Expansion test for RVEs of IM7/PEEK material at carbon fiber volume percent of 54.7 vol%.(left: Axial Strain, 1st middle: Axial Stress, 2nd Middle: von Mises Strain and right: von Mises Stress)

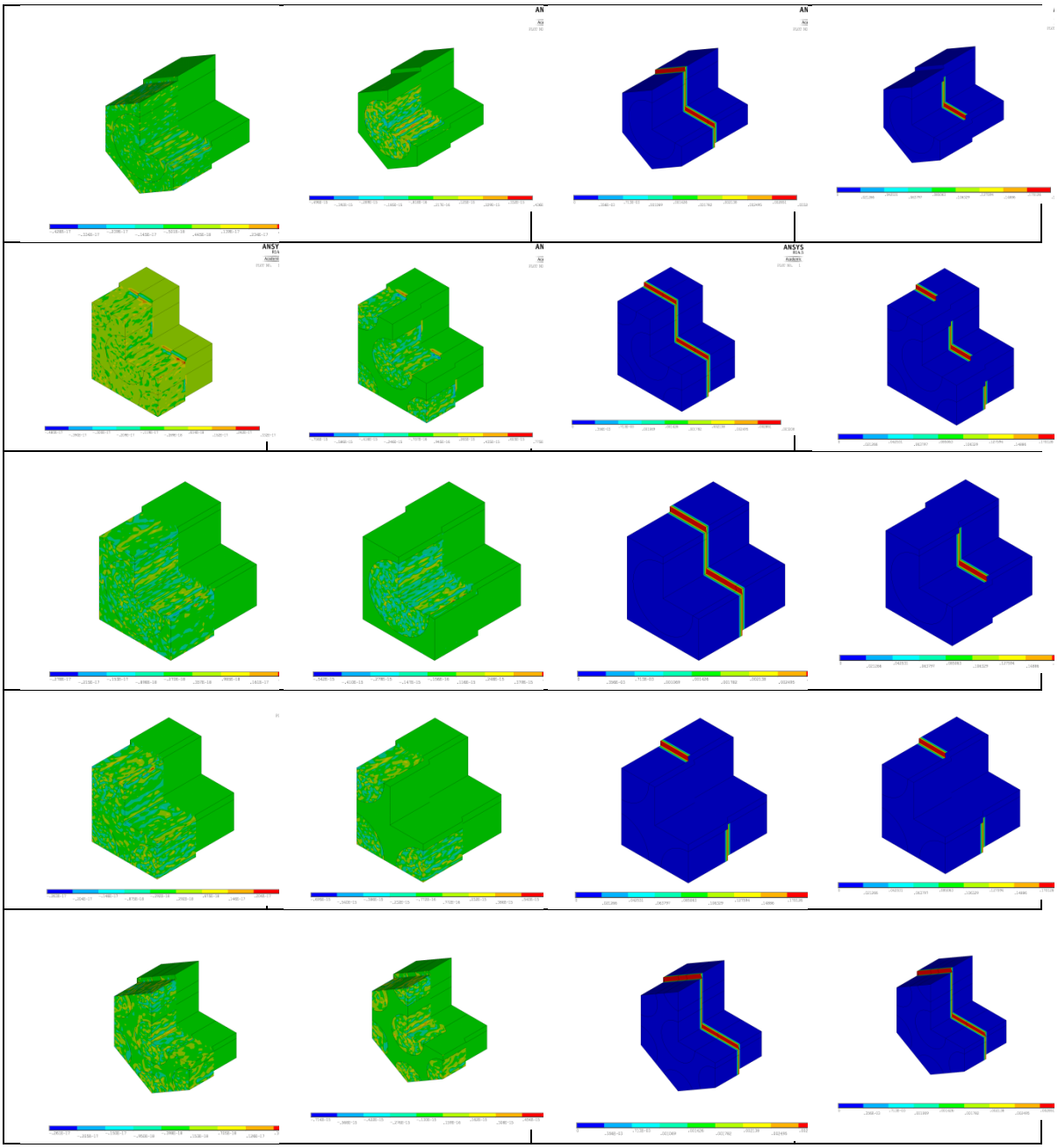

Figure 15: Shear test for RVEs of IM7/PEEK material at carbon fiber volume percent of 54.7 vol%.(left: Axial Strain, 1st middle: Axial Stress, 2nd Middle: von Mises Strain and right: von Mises Stress)

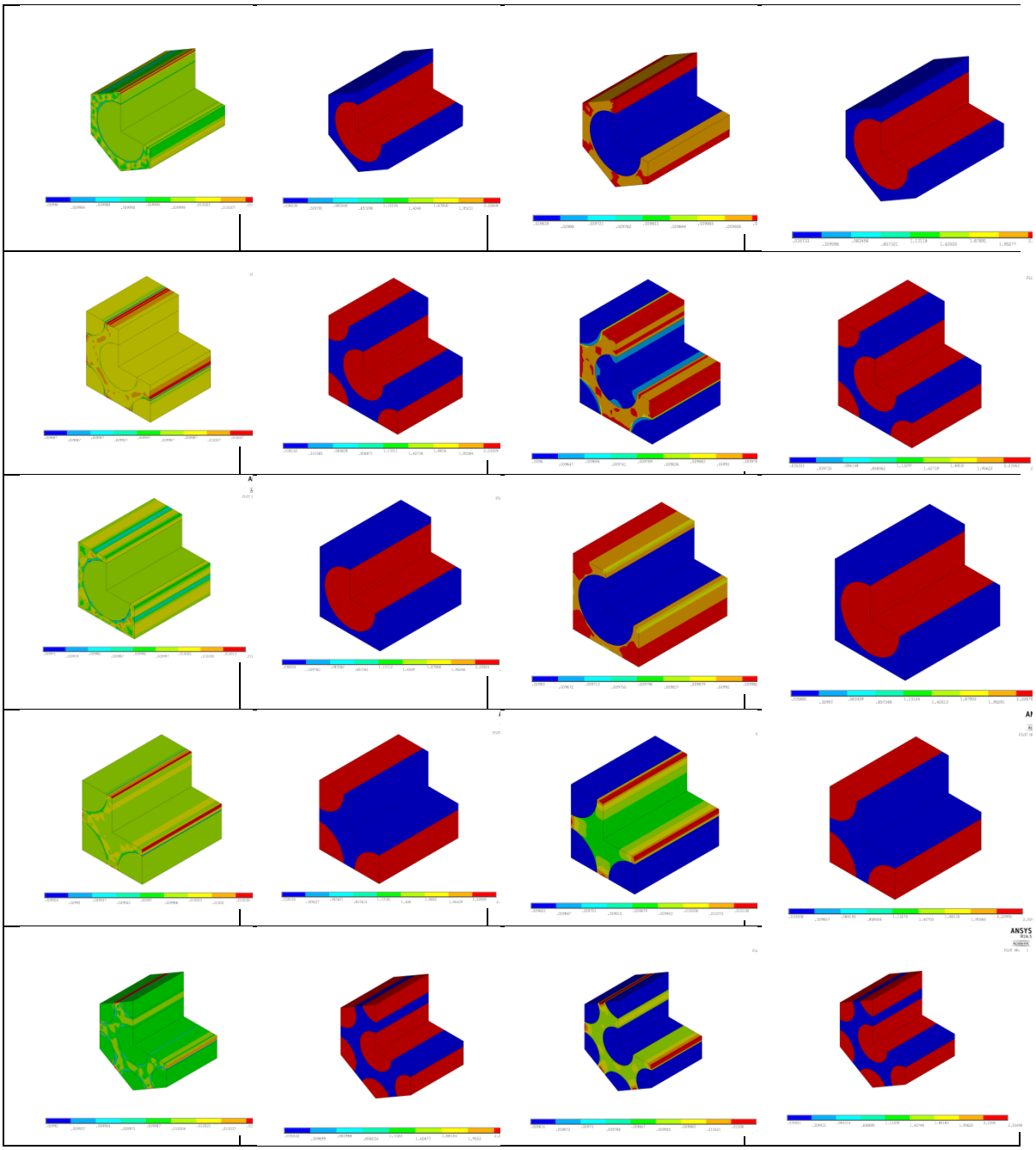

Figure 16: Tensile test for RVEs of IM7/PEEK material at carbon fiber volume percent of 54.7 vol%.(left: Axial Strain, 1st middle: Axial Stress, 2nd Middle: von Mises Strain and right: von Mises Stress).

The equivalent elastic properties of the RVEs extracted from modeling are listed in Table 2 and the average values are plotted in Fig. 16.

Table 2: Material properties of the RVEs of IM7/PEEK extracted from modeling (z-axis: fiber direction).

Vol %	RVEs	E_z	$E_x = E_y$	$G_{zx} = G_{zy}$	$\nu_{zx} = \nu_{zy}$	ν_{xy}	$\nu_{xz} = \nu_{yz}$	G_{xy}
30.000	SQ. Center	77.405	7.747	7.546	0.340	0.357	0.034	2.855
	SQ. Corner	77.403	7.966	7.546	0.338	0.357	0.035	2.935
	SQ. Center & Corner	77.312	7.968	7.539	0.338	0.357	0.035	2.936
	Hex. Center	77.369	7.613	7.543	0.348	0.357	0.034	2.805
	Hex. Center & Corner	76.944	8.015	7.508	0.345	0.357	0.036	2.953
	Mean	**77.286**	**7.862**	**7.537**	**0.342**	**0.357**	**0.035**	**2.897**
35.000	SQ. Center	89.705	8.192	8.584	0.337	0.357	0.031	3.020
	SQ. Corner	89.703	8.322	8.584	0.336	0.357	0.031	3.067
	SQ. Center & Corner	89.597	8.389	8.575	0.336	0.357	0.031	3.092
	Hex. Center	89.663	8.031	8.580	0.345	0.357	0.031	2.960
	Hex. Center & Corner	89.167	8.431	8.538	0.342	0.357	0.032	3.108
	Mean	**89.567**	**8.273**	**8.572**	**0.339**	**0.357**	**0.031**	**3.049**
40.000	SQ. Center	102.005	8.669	9.621	0.334	0.356	0.028	3.197
	SQ. Corner	102.004	8.713	9.621	0.334	0.356	0.029	3.213
	SQ. Center & Corner	101.882	8.836	9.610	0.333	0.356	0.029	3.258
	Hex. Center	101.957	8.475	9.617	0.342	0.356	0.028	3.125
	Hex. Center & Corner	101.668	8.929	9.592	0.339	0.356	0.030	3.292
	Mean	**101.903**	**8.724**	**9.612**	**0.336**	**0.356**	**0.029**	**3.217**
45.000	SQ. Center	114.306	9.184	10.658	0.331	0.356	0.027	3.388
	SQ. Corner	114.305	9.153	10.658	0.331	0.356	0.027	3.376
	SQ. Center & Corner	114.167	9.317	10.646	0.330	0.356	0.027	3.437
	Hex. Center	114.251	8.955	10.653	0.339	0.356	0.027	3.495
	Hex. Center & Corner	113.927	9.416	10.626	0.337	0.356	0.028	3.473
	Mean	**114.191**	**9.205**	**10.648**	**0.334**	**0.356**	**0.027**	**3.434**
50.000	SQ. Center	126.606	9.742	11.695	0.328	0.355	0.025	3.595
	SQ. Corner	126.605	9.664	11.695	0.328	0.355	0.025	3.566
	SQ. Center & Corner	126.451	9.842	11.682	0.328	0.355	0.025	3.632
	Hex. Center	126.546	9.470	11.690	0.336	0.355	0.025	3.690
	Hex. Center & Corner	126.185	10.034	11.660	0.333	0.355	0.027	3.702
	Mean	**126.479**	**9.750**	**11.684**	**0.331**	**0.355**	**0.025**	**3.637**
54.700	SQ. Center	138.168	10.318	12.670	0.325	0.355	0.024	3.809
	SQ. Corner	138.168	10.239	12.670	0.326	0.355	0.024	3.780

	SQ. Center & Corner	137.999	10.379	12.656	0.325	0.355	0.024	3.831
	Hex. Center	138.102	9.995	12.664	0.333	0.355	0.024	3.703
	Hex. Center & Corner	137.708	10.713	12.631	0.331	0.355	0.026	3.955
	Mean	**138.029**	**10.329**	**12.658**	**0.328**	**0.355**	**0.025**	**3.815**
55.000	SQ. Center	138.906	10.356	12.732	0.325	0.355	0.024	3.823
	SQ. Corner	138.906	10.272	12.732	0.326	0.355	0.024	3.792
	SQ. Center & Corner	138.736	10.414	12.718	0.325	0.355	0.024	3.844
	Hex. Center	138.840	10.030	12.727	0.333	0.355	0.024	3.933
	Hex. Center & Corner	138.443	10.751	12.693	0.330	0.355	0.026	3.969
	Mean	**138.766**	**10.365**	**12.720**	**0.328**	**0.355**	**0.024**	**3.872**
60.000	SQ. Center	151.206	11.032	13.769	0.322	0.354	0.024	4.074
	SQ. Corner	151.207	11.017	13.769	0.322	0.354	0.023	4.068
	SQ. Center & Corner	151.021	11.047	13.754	0.322	0.354	0.024	4.079
	Hex. Center	151.134	10.651	13.763	0.330	0.354	0.023	4.187
	Hex. Center & Corner	150.702	11.409	13.727	0.327	0.354	0.025	4.213
	Mean	**151.054**	**11.031**	**13.757**	**0.325**	**0.354**	**0.024**	**4.124**
65.000	SQ. Center	163.506	11.783	14.807	0.320	0.354	0.023	4.353
	SQ. Corner	163.507	11.943	14.807	0.319	0.354	0.023	4.412
	SQ. Center & Corner	163.306	11.747	14.790	0.320	0.354	0.023	4.340
	Hex. Center	163.428	11.334	14.800	0.328	0.354	0.023	4.187
	Hex. Center & Corner	162.960	12.179	14.760	0.325	0.354	0.024	4.499
	Mean	**163.341**	**11.797**	**14.793**	**0.322**	**0.354**	**0.023**	**4.358**
70.000	SQ. Center	175.805	12.621	15.844	0.317	0.353	0.023	4.664
	SQ. Corner	175.808	13.102	15.844	0.316	0.353	0.024	4.842
	SQ. Center & Corner	175.591	12.539	15.826	0.317	0.353	0.023	4.634
	Hex. Center	175.721	12.082	15.837	0.325	0.353	0.022	4.465
	Hex. Center & Corner	175.218	13.057	15.794	0.322	0.353	0.024	4.825
	Mean	**175.629**	**12.680**	**15.829**	**0.319**	**0.353**	**0.023**	**4.686**

a)

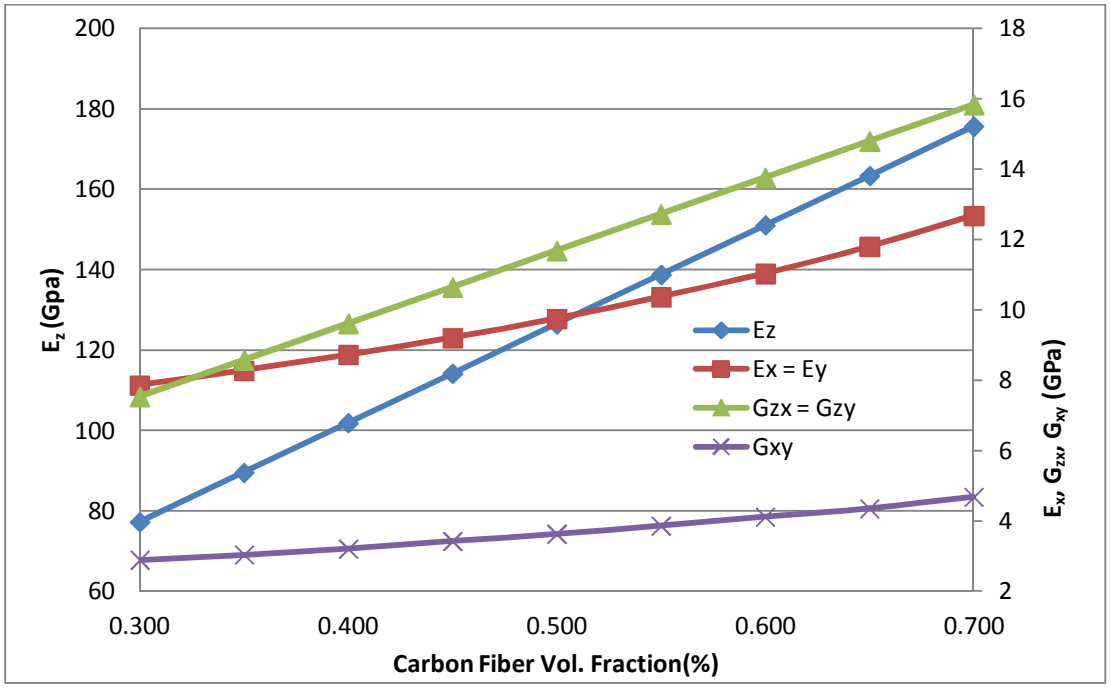

(b)

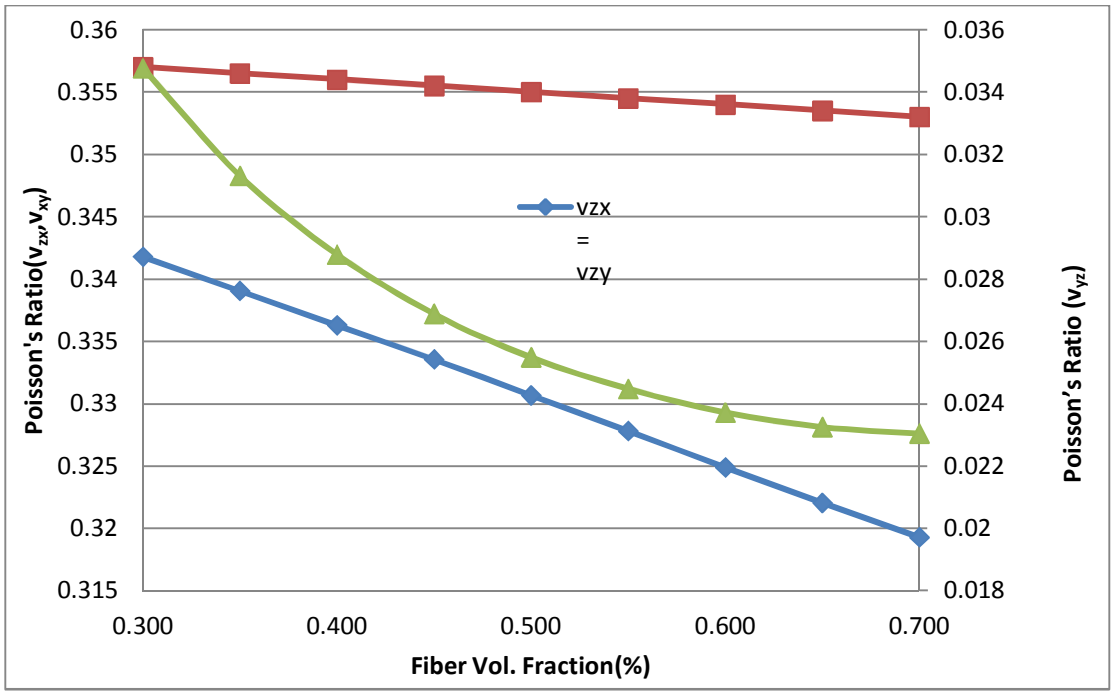

Figure 17: Material properties of the RVEs of IM7/PEEK extracted from modeling. (a) Young's moduli, Ex and Ez, and shear moduli, Gxy and Gzx, and (b) Poisson's ratios vxy, vyz, and vzx.

Table 3: Comparison of material properties of the IM7/PEEK uni-directional carbon fiber composites (carbon fiber of 54.7 vol %) by modeling and experiments (z-axis: fiber direction).

	Vol (%)	E_z (GPa)	E_x (GPa)	G_{zx} (GPa)	ν_{zx}	ν_{xy}	ν_{yz}	G_{xy}
Modeling	54.700	138.029	10.329	12.658	0.328	0.355	0.025	3.815
Experiment	54.700	139.420	9.349	9.290	0.330	_	_	_
Difference (%)		1.003	9.961	15.347	0.598			

5.2 Case Study-2:

For measuring the carbon fiber diameters and volume fraction, the samples were cut from the composite plate by water jet machine and molded and polished, and then Keyence VHX-600 Digital Microscope were used for measurements. The average fiber diameter was found to be 6.6 μm and the fiber volume percentage is 52.65%.The material elastic properties of carbon fibers and epoxy are listed in Table 4.

Table 4: Material properties of carbon fiber and epoxy

Material	$E_x=E_y$ (GPa)	E_z (GPa)	$\nu_{xy}=\nu_{yx}$	$\nu_{zx}=\nu_{zy}$	$\nu_{xz}=\nu_{yz}$	G_{xy} (GPa)	G_{zx} (GPa)
Carbon Fiber	22.4	250	0.35	0.30	0.027	8.30	22.1
Epoxy	2.03	2.03	0.4	0.4	0.4	0.725	0.725

Using the similar way to evaluate the effective mechanical properties of the carbon fiber CF/Epoxy 3D orthogonal fabric composites, in the first step, the square and hexagonal RVEs with a continuous carbon fiber in the matrix in each RVE is studies. Epoxy is considered as the matrix material. The deformation and stresses are modeled and computed for the three test cases to extract the equivalent material constants for the RVEs using afore described equations. The commercial FEA software ANSYS® was used for modeling. The FEA models for different RVEs are shown in Fig.9. Eight-node 3D solid structure elements of SOLID185 are employed. The proper element size and element

density distribution, total elements, and total nodes are determined through convergence study of the extracted material properties and stress-strain distributions so that the modeling results are mesh-independent.

In step one, the equivalent elastic properties of the RVEs extracted from modeling are listed in Table.5 and the average values are plotted in Fig. 17. The data from these five RVEs are very close and representative. Therefore, the averaged data for these five RVEs represent the equivalent elastic properties of the micro-heterostructures of the composites reinforced by carbon fibers. The average equivalent Young's modulus, E_z, and shear modulus, G_{zx}, linearly increase as carbon fiber volume fraction increases, which can be well predicted by the rule of mixture, as shown in Fig. 17.

Table 5 : Material properties of the RVEs of Carbon Fiber/Epoxy extracted from modeling (z-axis: fiber direction).

Vol %	RVEs	E_z (GPa)	$E_x = E_y$ (GPa)	$G_{zx} = G_{zy}$ (GPa)	$\nu_{zx} = \nu_{zy}$	ν_{xy}	$\nu_{xz} = \nu_{yz}$	G_{xy} (GPa)
30	SQ. Center	76.304	5.807068154	7.12333709	0.367378	0.385	0.027959087	2.096414496
	SQ. Corner	76.301	6.003163197	7.12333709	0.364195	0.385	0.02865391	2.16720693
	SQ. Center & Corner	76.21	5.996771658	7.115338718	0.364374	0.385	0.028671693	2.164899516
	Hex. Center	76.2677	5.697756405	7.120190333	0.376405	0.385	0.028120184	2.056951771
	Hex. Center & Corner	75.8395	6.017795668	7.083425578	0.371144	0.385	0.029449936	2.172489411
	Mean	**76.18444**	**5.904511016**	**7.113125762**	**0.368699**	**0.385**	**0.028570962**	**2.131592425**
35	SQ. Center	88.683	6.193886389	8.190013148	0.362229	0.3825	0.025299166	2.240103576
	SQ. Corner	88.681	6.321440273	8.190013148	0.360409	0.3825	0.025690994	2.28623518
	SQ. Center & Corner	88.574	6.366191399	8.180681714	0.359818	0.3825	0.025861686	2.302420036
	Hex. Center	88.6408	6.058718041	8.186341932	0.371389	0.3825	0.025384913	2.191218098
	Hex. Center & Corner	88.1415	6.381808279	8.143449718	0.366642	0.3825	0.026546392	2.308068094
	Mean	**88.54406**	**6.264408876**	**8.178099932**	**0.364097**	**0.3825**	**0.02575663**	**2.265608997**
40	SQ. Center	101.062	6.616703972	9.256689206	0.357185	0.38	0.02338555	2.397356512
	SQ. Corner	101.06	6.675331826	9.256689206	0.356321	0.38	0.0235361	2.418598488
	SQ. Center & Corner	100.937	6.767163171	9.24602471	0.355308	0.38	0.023821062	2.451870714
	Hex. Center	101.0137	6.450256214	9.25249353	0.366419	0.38	0.023397812	2.337049353
	Hex. Center & Corner	100.7226	6.818907379	9.227529844	0.362225	0.38	0.024522618	2.470618616
	Mean	**100.95906**	**6.665672512**	**9.247885299**	**0.359492**	**0.38**	**0.023732628**	**2.415098736**

45	SQ. Center	113.441	7.081028947	10.32336965	0.35225	0.3775	0.021987585	2.570246442
	SQ. Corner	113.44	7.082875072	10.32336965	0.35225	0.3775	0.021993511	2.570916542
	SQ. Center & Corner	113.301	7.205717012	10.31136551	0.350753	0.3775	0.022307195	2.615505267
	Hex. Center	113.3866	6.881763417	10.31863636	0.361485	0.3775	0.021939599	2.673913767
	Hex. Center & Corner	113.0594	7.258632319	10.29056098	0.357709	0.3775	0.02296564	2.634712275
	Mean	**113.3256**	**7.102003353**	**10.31346043**	**0.35489**	**0.3775**	**0.022238706**	**2.613058859**
50	SQ. Center	125.819	7.594642412	11.39004717	0.347373	0.375	0.020967981	2.76168815
	SQ. Corner	125.819	7.566613965	11.39004717	0.347614	0.375	0.020905135	2.751495987
	SQ. Center & Corner	125.664	7.691614719	11.37670924	0.346479	0.375	0.021207239	2.796950807
	Hex. Center	125.7592	7.35326286	11.38478796	0.356696	0.375	0.020856335	2.774358448
	Hex. Center & Corner	125.3961	7.819058882	11.35359309	0.352623	0.375	0.021987776	2.843294139
	Mean	**125.69146**	**7.605038568**	**11.37903693**	**0.350157**	**0.375**	**0.021184893**	**2.785557506**
52.65	SQ. Center	132.38	7.893052521	11.9553848	0.3448	0.373675	0.020558449	2.872969414
	SQ. Corner	132.381	7.865749856	11.9553848	0.345048	0.373675	0.02050192	2.863031596
	SQ. Center & Corner	132.217	7.972190539	11.94133997	0.343966	0.373675	0.020739863	2.901774633
	Hex. Center	132.3167	7.622133681	11.94984686	0.354179	0.373675	0.020402549	2.869026883
	Hex. Center & Corner	131.9346	8.198973308	11.91699867	0.3496	0.373675	0.021725626	2.984320639
	Mean	**132.24586**	**7.910419981**	**11.94379102**	**0.347519**	**0.373675**	**0.020785681**	**2.898224633**
55	SQ. Center	138.198	8.171161928	12.45672176	0.342524	0.3725	0.020252213	2.976743872
	SQ. Corner	138.199	8.157697105	12.45672176	0.342524	0.3725	0.020218694	2.971838654
	SQ. Center & Corner	138.027	8.235648472	12.44205005	0.342057	0.3725	0.020409492	3.000236238
	Hex. Center	138.1318	7.875478793	12.45093664	0.351955	0.3725	0.020066422	3.090825126
	Hex. Center & Corner	137.7328	8.476150979	12.41662228	0.347533	0.3725	0.021387361	3.087850994
	Mean	**138.05772**	**8.183227455**	**12.4446105**	**0.345318**	**0.3725**	**0.020466837**	**3.025498977**
60	SQ. Center	150.576	8.823650174	13.52339344	0.337894	0.37	0.019800336	3.220310283
	SQ. Corner	150.579	8.905462993	13.52339344	0.337099	0.37	0.019936543	3.250168975
	SQ. Center & Corner	150.391	8.847195674	13.50739669	0.337606	0.37	0.019860669	3.228903531
	Hex. Center	150.5042	8.468860846	13.51709992	0.347243	0.37	0.019539328	3.339718682
	Hex. Center & Corner	150.0693	9.108391055	13.4796544	0.34226	0.37	0.020773318	3.324230312
	Mean	**150.4239**	**8.830712148**	**13.51018758**	**0.34042**	**0.37**	**0.019982039**	**3.272666357**
65	SQ. Center	162.955	9.563993143	14.59006365	0.333224	0.3675	0.019557272	3.496889632
	SQ. Corner	162.958	9.875011908	14.59006365	0.331295	0.3675	0.020075983	3.610607645
	SQ. Center & Corner	162.754	9.547948734	14.57273385	0.333266	0.3675	0.019551043	3.491023303
	Hex. Center	162.8765	9.134130595	14.58324568	0.342565	0.3675	0.019211071	3.339718682
	Hex. Center & Corner	162.4058	9.871501163	14.54268602	0.337678	0.3675	0.020525083	3.609324008
	Mean	**162.78986**	**9.598517109**	**14.57575857**	**0.335606**	**0.3675**	**0.019784091**	**3.509512654**
70	SQ. Center	175.333	10.42016197	15.65674555	0.328642	0.365	0.01953141	3.816909145
	SQ. Corner	175.338	11.14726155	15.65674555	0.324923	0.365	0.020657284	4.08324599
	SQ. Center & Corner	175.118	10.34468458	15.63808269	0.328858	0.365	0.019426509	3.789261752
	Hex. Center	175.2487	9.885795886	15.64940312	0.338071	0.365	0.0190706	3.621170654
	Hex. Center & Corner	174.7422	10.76976001	15.60571667	0.333135	0.365	0.020531861	3.944967035

	Mean	175.15598	10.5135328	15.64133872	0.330726	0.365	0.019843533	3.851110915

(a)

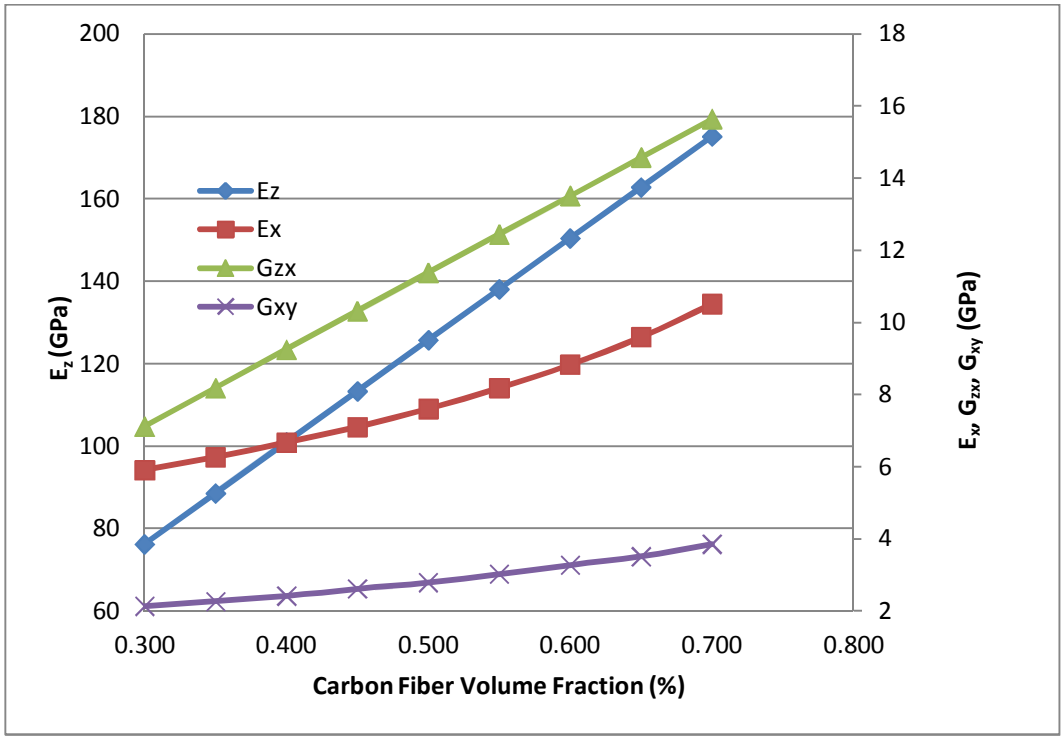

(b)

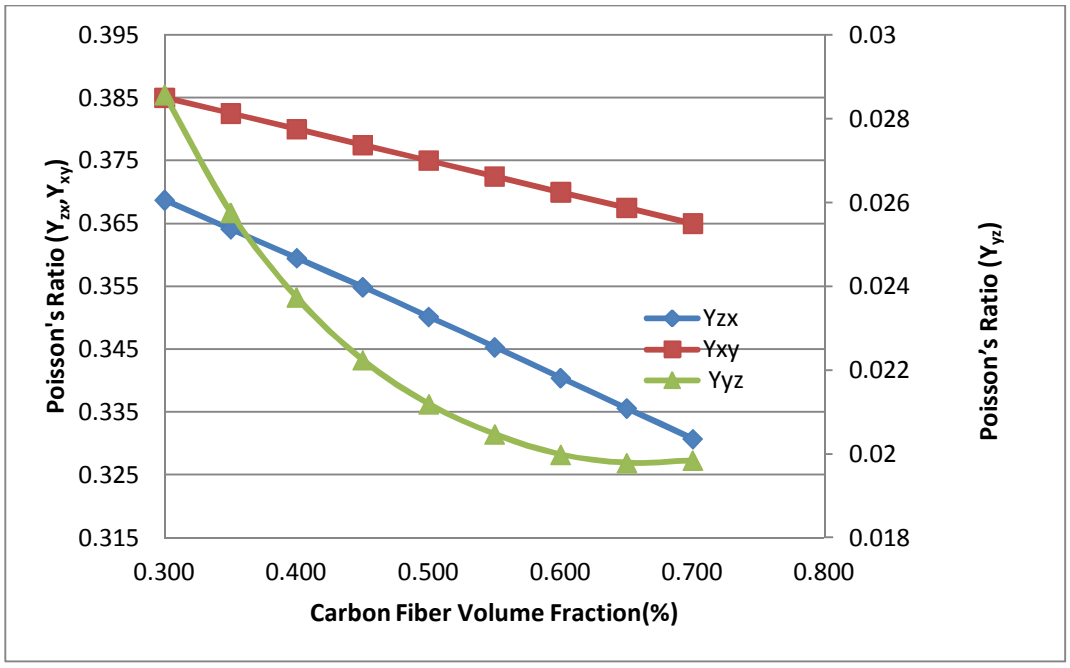

Figure 18: Material properties of the RVEs of Carbon Fiber/Epoxy extracted from modeling. (a) Young's moduli, Ex and Ez, and shear moduli, Gxy and Gzx, and (b) Poisson's ratios vxy, vyz, and vzx.

5.3 Case Study-3:

Like the case study.2, here we tried to predict the properties of carbon fiber reinforced by another polymer material Polyamide 6 or known as Nylon 6 through five different representative volume elements. For analyzing the RVE properties of the composite, the initial mechanical properties were taken as reference values.

Table 6: Material properties of carbon fiber and Polyamide 6 (z-axis: fiber direction).

Material	$E_x=E_y$ (GPa)	E_z (GPa)	$\nu_{xy}=\nu_{yx}$	$\nu_{zx}=\nu_{zy}$	$\nu_{xz}=\nu_{yz}$	G_{xy} (GPa)	G_{zx} (GPa)
Carbon Fiber	22.4	250	0.35	0.30	0.027	8.30	22.1
Polyamide 6	2.4784	2.4784	0.35	0.35	0.35	0.9179	0.9179

Using the similar way to evaluate the effective mechanical properties of the carbon fiber CF/polyamide 6 3D orthogonal fabric composites, in the first step, the square and hexagonal RVEs with a continuous carbon fiber in the matrix in each RVE is studies. Epoxy is considered as the matrix material. The deformation and stresses are modeled and computed for the three test cases to extract the equivalent material constants for the RVEs using afore described equations. The commercial FEA software ANSYS® was used for modeling. The FEA models for different RVEs are shown in Fig.9. Eight-node 3D solid structure elements of SOLID185 are employed. The proper element size and element density distribution, total elements, and total nodes are determined through convergence study of the extracted material properties and stress-strain distributions so that the modeling results are mesh-independent.

In step one, the equivalent elastic properties of the RVEs extracted from modeling are listed in Table.7 and the average values are plotted in Fig. 18. The data from these five

RVEs are very close and representative. Therefore, the averaged data for these five RVEs represent the equivalent elastic properties of the micro-heterostructures of the composites reinforced by carbon fibers. The average equivalent Young's modulus, E_z, and shear modulus, G_{zx}, linearly increase as carbon fiber volume fraction increases, which can be well predicted by the rule of mixture, as shown in Fig.16(a).

Table 7: Material properties of the RVEs of Carbon Fiber/Polyamide 6 extracted from modeling (z-axis: fiber direction).

Vol %	RVEs	E_z (GPa)	$E_x = E_y$ (GPa)	$G_{zx} = G_{zy}$ (GPa)	$\nu_{zx} = \nu_{zy}$	ν_{xy}	$\nu_{xz} = \nu_{yz}$	G_{xy} (GPa)
30.000	SQ. Center	76.617	5.401	7.262	0.333	0.350	0.023	2.000
	SQ. Corner	76.616	5.554	7.262	0.332	0.350	0.024	2.057
	SQ. Center & Corner	76.524	5.572	7.254	0.332	0.350	0.024	2.064
	Hex. Center	76.581	5.300	7.259	0.334	0.350	0.023	1.963
	Hex. Center & Corner	76.155	5.608	7.223	0.331	0.350	0.024	2.077
	Mean	**76.498**	**5.487**	**7.252**	**0.332**	**0.350**	**0.024**	**2.032**
35.000	SQ. Center	88.974	5.758	8.320	0.330	0.350	0.021	2.133
	SQ. Corner	88.973	5.842	8.320	0.330	0.350	0.022	2.164
	SQ. Center & Corner	88.865	5.911	8.310	0.329	0.350	0.022	2.189
	Hex. Center	88.931	5.631	8.316	0.331	0.350	0.021	2.086
	Hex. Center & Corner	88.434	5.941	8.274	0.329	0.350	0.022	2.200
	Mean	**88.835**	**5.817**	**8.308**	**0.330**	**0.350**	**0.022**	**2.154**
40.000	SQ. Center	101.330	6.149	9.377	0.328	0.350	0.020	2.277
	SQ. Corner	101.329	6.167	9.377	0.328	0.350	0.020	2.284
	SQ. Center & Corner	101.206	6.280	9.367	0.327	0.350	0.020	2.326
	Hex. Center	101.281	5.992	9.373	0.329	0.350	0.019	2.219
	Hex. Center & Corner	100.992	6.353	9.348	0.327	0.350	0.021	2.353
	Mean	**101.228**	**6.188**	**9.368**	**0.328**	**0.350**	**0.020**	**2.292**
45.000	SQ. Center	113.686	6.581	10.435	0.325	0.350	0.019	2.437
	SQ. Corner	113.686	6.547	10.435	0.325	0.350	0.019	2.425
	SQ. Center & Corner	113.547	6.689	10.423	0.325	0.350	0.019	2.477
	Hex. Center	113.632	6.393	10.430	0.326	0.350	0.018	2.531
	Hex. Center & Corner	113.306	6.767	10.402	0.325	0.350	0.019	2.506
	Mean	**113.571**	**6.595**	**10.425**	**0.325**	**0.350**	**0.019**	**2.475**
50.000	SQ. Center	126.042	7.063	11.492	0.323	0.350	0.018	2.616
	SQ. Corner	126.042	7.003	11.492	0.323	0.350	0.018	2.594
	SQ. Center & Corner	125.888	7.144	11.479	0.323	0.350	0.018	2.646

	Hex. Center	125.982	6.834	11.487	0.324	0.350	0.018	2.701
	Hex. Center & Corner	125.620	7.306	11.456	0.322	0.350	0.019	2.706
	Mean	**125.915**	**7.070**	**11.481**	**0.323**	**0.350**	**0.018**	**2.653**
54.700	SQ. Center	137.657	7.568	12.486	0.321	0.350	0.018	2.803
	SQ. Corner	132.591	7.524	12.486	0.328	0.350	0.019	2.787
	SQ. Center & Corner	132.428	7.615	12.507	0.328	0.350	0.019	2.820
	Hex. Center	137.591	7.294	12.480	0.322	0.350	0.017	2.712
	Hex. Center & Corner	137.195	7.916	12.446	0.320	0.350	0.018	2.932
	Mean	**135.492**	**7.583**	**12.481**	**0.324**	**0.350**	**0.018**	**2.811**
55.000	SQ. Center	138.398	7.603	12.549	0.321	0.350	0.018	2.816
	SQ. Corner	138.398	7.566	12.549	0.321	0.350	0.018	2.802
	SQ. Center & Corner	138.228	7.658	12.535	0.320	0.350	0.018	2.836
	Hex. Center	138.332	7.321	12.544	0.322	0.350	0.017	2.918
	Hex. Center & Corner	137.934	7.952	12.510	0.320	0.350	0.018	2.945
	Mean	**138.258**	**7.620**	**12.537**	**0.321**	**0.350**	**0.018**	**2.863**
60.000	SQ. Center	150.754	8.217	13.607	0.318	0.350	0.017	3.043
	SQ. Corner	150.755	8.286	13.607	0.318	0.350	0.017	3.069
	SQ. Center & Corner	150.569	8.242	13.591	0.318	0.350	0.017	3.053
	Hex. Center	150.682	7.878	13.601	0.320	0.350	0.017	3.150
	Hex. Center & Corner	150.248	8.565	13.563	0.317	0.350	0.018	3.172
	Mean	**150.602**	**8.238**	**13.594**	**0.318**	**0.350**	**0.017**	**3.097**
65.000	SQ. Center	163.110	8.918	14.664	0.316	0.350	0.017	3.303
	SQ. Corner	163.111	9.230	14.664	0.315	0.350	0.018	3.418
	SQ. Center & Corner	162.910	8.914	14.647	0.316	0.350	0.017	3.301
	Hex. Center	163.032	8.504	14.657	0.317	0.350	0.017	3.150
	Hex. Center & Corner	162.562	9.316	14.617	0.315	0.350	0.018	3.450
	Mean	**162.945**	**8.976**	**14.650**	**0.316**	**0.350**	**0.017**	**3.325**
70.000	SQ. Center	175.466	9.734	15.722	0.314	0.350	0.017	3.605
	SQ. Corner	175.468	10.493	15.722	0.312	0.350	0.019	3.886
	SQ. Center & Corner	175.251	9.709	15.703	0.314	0.350	0.017	3.596
	Hex. Center	175.382	9.220	15.714	0.315	0.350	0.017	3.415
	Hex. Center & Corner	174.876	10.207	15.671	0.313	0.350	0.018	3.780
	Mean	**175.289**	**9.872**	**15.706**	**0.314**	**0.350**	**0.018**	**3.656**

(a)

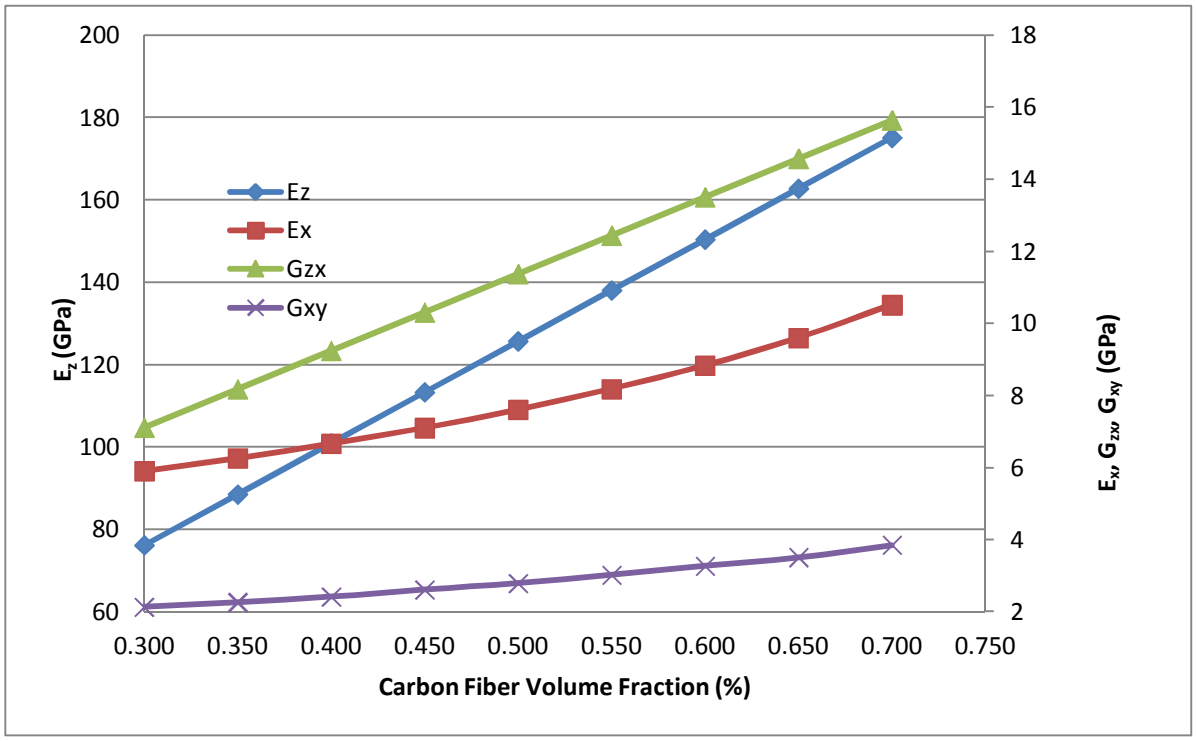

(b)

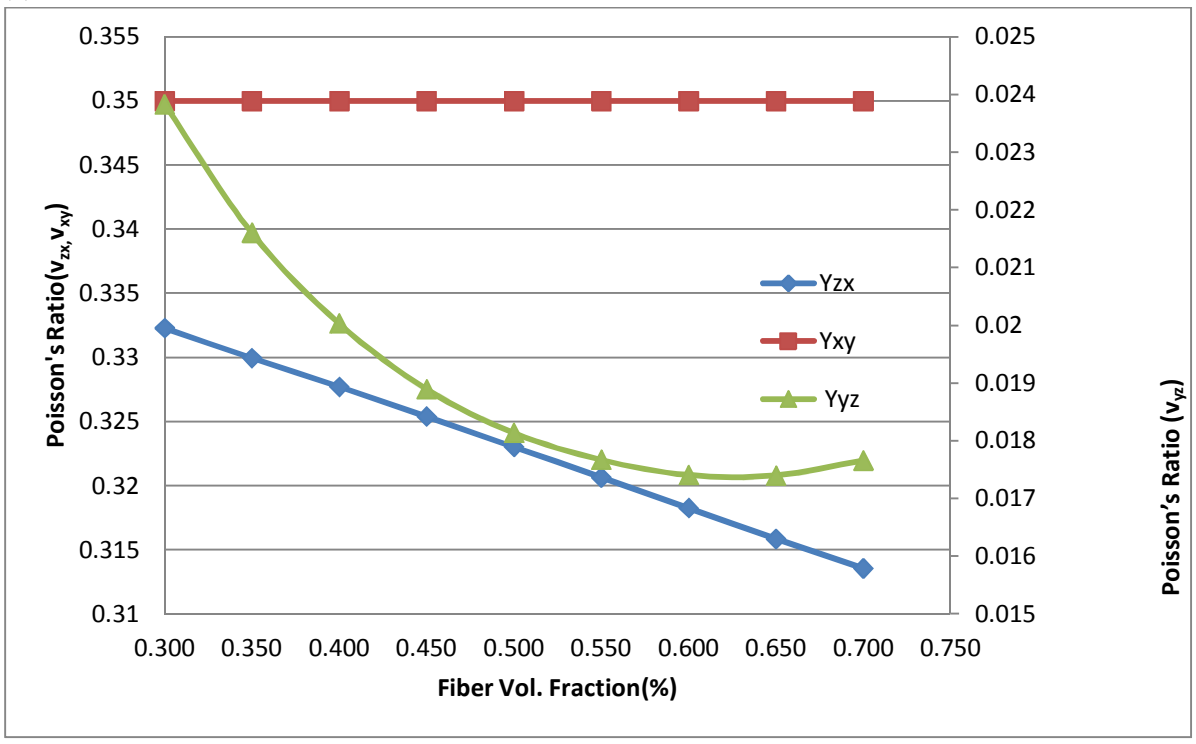

Figure 19: Material properties of the RVEs of Carbon Fiber/Polyamide 6 extracted from modeling. (a) Young's moduli, Ex and Ez, and shear moduli, Gxy and Gzx, and (b) Poisson's ratios vxy, vyz, and vzx.

5.4 Case Study-4:

Like the case study.2, here we tried to predict the properties of glass fiber reinforced by another polymer material epoxy through five different representative volume elements. For analyzing the RVE properties of the composite, the initial mechanical properties were taken as reference values.

Table 8: Material properties of glass fiber and Epoxy (z-axis: fiber direction).

Material	$E_x=E_y$ (GPa)	E_z (GPa)	$\nu_{xy}=\nu_{yx}$	$\nu_{zx}=\nu_{zy}$	$\nu_{xz}=\nu_{yz}$	G_{xy} (GPa)	G_{zx} (GPa)
Glass Fiber	86	86	0.2	0.2	0.2	35.8	35.8
Epoxy	3.5	3.5	0.35	0.35	0.35	1.29	1.29

Using the similar way to evaluate the effective mechanical properties of the Glass Fiber/Epoxy 3D orthogonal fabric composites, in the first step, the square and hexagonal RVEs with a continuous carbon fiber in the matrix in each RVE is studies. Epoxy is considered as the matrix material. The deformation and stresses are modeled and computed for the three test cases to extract the equivalent material constants for the RVEs using afore described equations. The commercial FEA software ANSYS® was used for modeling. The FEA models for different RVEs are shown in Fig.9. Eight-node 3D solid structure elements of SOLID185 are employed. The proper element size and element density distribution, total elements, and total nodes are determined through convergence study of the extracted material properties and stress-strain distributions so that the modeling results are mesh-independent.

In step one, the equivalent elastic properties of the RVEs extracted from modeling are listed in Table.9 and the average values are plotted in Fig. 19. The data from these five

RVEs are very close and representative. Therefore, the averaged data for these five RVEs represent the equivalent elastic properties of the micro-heterostructures of the composites reinforced by carbon fibers. The average equivalent Young's modulus, E_z, and shear modulus, G_{zx}, linearly increase as glass fiber volume fraction increases, which can be well predicted by the rule of mixture, as shown in Fig.19.

Table 9: Material properties of the RVEs of Glass Fiber/Epoxy extracted from modeling (z-axis: fiber direction).

Vol %	RVEs	E_z	$E_x = E_y$	$G_{zx} = G_{zy}$	$\nu_{zx} = \nu_{zy}$	ν_{xy}	$\nu_{xz} = \nu_{yz}$	G_{xy}
0.500	SQ. Center	3.903	3.666	1.465	0.349	0.349	0.328	1.359
	SQ. Corner	3.902	3.667	1.465	0.349	0.349	0.328	1.359
	SQ. Center & Corner	3.902	3.670	1.465	0.349	0.349	0.328	1.360
	Hex. Center	3.903	3.614	1.465	0.356	0.349	0.330	1.339
	Hex. Center & Corner	3.863	3.652	1.448	0.354	0.349	0.334	1.354
	Mean	**3.895**	**3.654**	**1.461**	**0.351**	**0.349**	**0.330**	**1.354**
5.000	SQ. Center	7.583	4.707	3.003	0.341	0.343	0.211	1.753
	SQ. Corner	7.580	4.600	3.003	0.344	0.343	0.209	1.713
	SQ. Center & Corner	7.582	4.678	3.003	0.342	0.343	0.211	1.742
	Hex. Center	7.525	4.638	2.979	0.348	0.343	0.215	1.727
	Hex. Center & Corner	7.500	4.792	2.970	0.342	0.343	0.219	1.785
	Mean	**7.554**	**4.683**	**2.992**	**0.343**	**0.343**	**0.213**	**1.744**
10.000	SQ. Center	11.666	5.473	4.711	0.332	0.335	0.156	2.050
	SQ. Corner	11.659	5.163	4.711	0.340	0.335	0.151	1.934
	SQ. Center & Corner	11.663	5.360	4.711	0.335	0.335	0.154	2.008
	Hex. Center	11.549	5.384	4.662	0.340	0.335	0.158	2.017
	Hex. Center & Corner	11.500	5.562	4.643	0.334	0.335	0.162	2.083
	Mean	**11.607**	**5.389**	**4.687**	**0.336**	**0.335**	**0.156**	**2.018**
15.000	SQ. Center	15.748	6.133	6.418	0.323	0.328	0.126	2.310
	SQ. Corner	15.739	5.613	6.418	0.336	0.328	0.120	2.114
	SQ. Center & Corner	15.805	5.990	6.444	0.326	0.328	0.124	2.256
	Hex. Center	15.748	6.039	6.418	0.331	0.328	0.127	2.274
	Hex. Center & Corner	15.712	6.263	6.405	0.325	0.328	0.130	2.359
	Mean	**15.750**	**6.007**	**6.420**	**0.328**	**0.328**	**0.125**	**2.263**
20.000	SQ. Center	19.829	6.778	8.125	0.315	0.320	0.108	2.567
	SQ. Corner	19.819	6.001	8.125	0.331	0.320	0.100	2.273
	SQ. Center & Corner	19.906	6.532	8.159	0.319	0.320	0.105	2.474

	Hex. Center	19.829	6.653	8.125	0.323	0.320	0.108	2.520
	Hex. Center & Corner	19.782	6.869	8.108	0.318	0.320	0.110	2.602
	Mean	**19.833**	**6.567**	**8.128**	**0.321**	**0.320**	**0.106**	**2.487**
25.000	SQ. Center	23.909	7.448	9.832	0.306	0.313	0.095	2.837
	SQ. Corner	23.899	6.416	9.832	0.326	0.313	0.087	2.444
	SQ. Center & Corner	24.007	7.099	9.875	0.312	0.313	0.092	2.705
	Hex. Center	24.060	7.305	9.895	0.314	0.313	0.095	2.783
	Hex. Center & Corner	23.977	7.558	9.863	0.309	0.313	0.097	2.879
	Mean	**23.970**	**7.165**	**9.860**	**0.314**	**0.313**	**0.094**	**2.730**
30.000	SQ. Center	28.231	8.192	11.641	0.298	0.305	0.086	3.139
	SQ. Corner	28.221	8.422	11.641	0.295	0.305	0.088	3.227
	SQ. Center & Corner	28.196	8.476	11.628	0.294	0.305	0.088	3.248
	Hex. Center	28.220	7.988	11.636	0.307	0.305	0.087	3.060
	Hex. Center & Corner	28.072	8.468	11.576	0.300	0.305	0.090	3.244
	Mean	**28.188**	**8.309**	**11.624**	**0.299**	**0.305**	**0.088**	**3.184**
35.000	SQ. Center	32.350	8.989	13.365	0.290	0.298	0.081	3.464
	SQ. Corner	32.342	9.110	13.365	0.289	0.298	0.081	3.511
	SQ. Center & Corner	32.310	9.253	13.350	0.287	0.298	0.082	3.566
	Hex. Center	32.338	8.730	13.359	0.299	0.298	0.081	3.364
	Hex. Center & Corner	32.166	9.231	13.290	0.293	0.298	0.084	3.557
	Mean	**32.301**	**9.063**	**13.346**	**0.292**	**0.298**	**0.082**	**3.492**
40.000	SQ. Center	36.469	9.879	15.089	0.283	0.290	0.077	3.829
	SQ. Corner	36.463	9.899	15.089	0.282	0.290	0.077	3.837
	SQ. Center & Corner	36.424	10.115	15.072	0.280	0.290	0.078	3.921
	Hex. Center	36.455	9.549	15.082	0.291	0.290	0.076	3.701
	Hex. Center & Corner	36.260	10.089	15.003	0.286	0.290	0.080	3.910
	Mean	**36.414**	**9.906**	**15.067**	**0.285**	**0.290**	**0.077**	**3.840**
45.000	SQ. Center	40.588	10.883	16.813	0.275	0.283	0.074	4.243
	SQ. Corner	40.584	10.838	16.813	0.276	0.283	0.074	4.225
	SQ. Center & Corner	40.538	11.091	16.794	0.274	0.283	0.075	4.324
	Hex. Center	40.572	10.476	16.805	0.284	0.283	0.073	4.521
	Hex. Center & Corner	40.354	11.063	16.716	0.279	0.283	0.076	4.313
	Mean	**40.527**	**10.870**	**16.788**	**0.277**	**0.283**	**0.074**	**4.325**
50.000	SQ. Center	44.705	12.035	18.537	0.268	0.275	0.072	4.720
	SQ. Corner	44.705	11.995	18.537	0.268	0.275	0.072	4.704
	SQ. Center & Corner	44.652	12.208	18.516	0.267	0.275	0.073	4.788
	Hex. Center	44.688	11.528	18.529	0.277	0.275	0.071	4.521
	Hex. Center & Corner	44.448	12.200	18.430	0.272	0.275	0.075	4.784
	Mean	**44.639**	**11.993**	**18.510**	**0.270**	**0.275**	**0.073**	**4.703**
55.000	SQ. Center	48.822	13.368	20.261	0.261	0.268	0.071	5.273
	SQ. Corner	48.827	13.477	20.261	0.260	0.268	0.072	5.316

	SQ. Center & Corner	48.765	13.510	20.237	0.260	0.268	0.072	5.330
	Hex. Center	48.803	12.743	20.252	0.270	0.268	0.070	5.614
	Hex. Center & Corner	48.541	13.537	20.143	0.265	0.268	0.074	5.340
	Mean	**48.752**	**13.327**	**20.231**	**0.263**	**0.268**	**0.072**	**5.375**
60.000	SQ. Center	52.939	14.938	21.985	0.254	0.260	0.072	5.928
	SQ. Corner	52.948	15.455	21.985	0.252	0.260	0.074	6.133
	SQ. Center & Corner	52.878	15.063	21.959	0.254	0.260	0.072	5.977
	Hex. Center	52.918	14.148	21.975	0.263	0.260	0.070	6.312
	Hex. Center & Corner	52.634	15.141	21.856	0.258	0.260	0.074	6.008
	Mean	**52.863**	**14.949**	**21.952**	**0.256**	**0.260**	**0.072**	**6.072**
65.000	SQ. Center	57.056	16.817	23.709	0.247	0.253	0.073	6.713
	SQ. Corner	57.070	18.248	23.709	0.243	0.253	0.078	7.285
	SQ. Center & Corner	56.992	16.945	23.681	0.247	0.253	0.073	6.765
	Hex. Center	57.033	15.813	23.698	0.256	0.253	0.071	6.312
	Hex. Center & Corner	56.726	17.148	23.570	0.251	0.253	0.076	6.845
	Mean	**56.975**	**16.994**	**23.674**	**0.249**	**0.253**	**0.074**	**6.784**
70.000	SQ. Center	61.172	19.110	25.433	0.241	0.245	0.075	7.675
	SQ. Corner	61.192	22.540	25.433	0.233	0.245	0.086	9.052
	SQ. Center & Corner	61.106	19.345	25.403	0.240	0.245	0.076	7.769
	Hex. Center	61.147	17.795	25.422	0.250	0.245	0.073	7.147
	Hex. Center & Corner	60.818	19.731	25.283	0.244	0.245	0.079	7.924
	Mean	**61.087**	**19.704**	**25.395**	**0.241**	**0.245**	**0.078**	**7.913**
75.000	SQ. Center	65.287	22.732	27.157	0.233	0.238	0.081	9.184
	SQ. Corner	65.317	29.824	27.157	0.222	0.238	0.101	12.050
	SQ. Center & Corner	65.221	22.544	27.125	0.233	0.238	0.081	9.109
	Hex. Center	65.261	20.187	27.145	0.243	0.238	0.075	8.157
	Hex. Center & Corner	64.910	23.168	26.996	0.237	0.238	0.084	9.361
	Mean	**65.199**	**23.691**	**27.116**	**0.234**	**0.238**	**0.085**	**9.572**

(a)

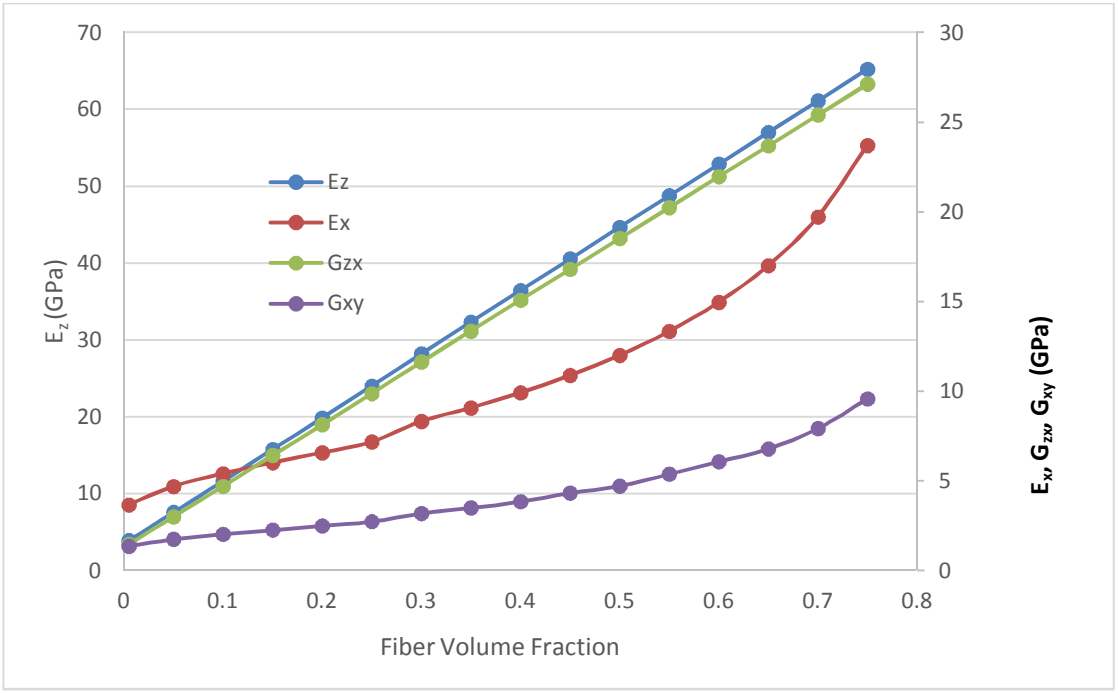

(b)

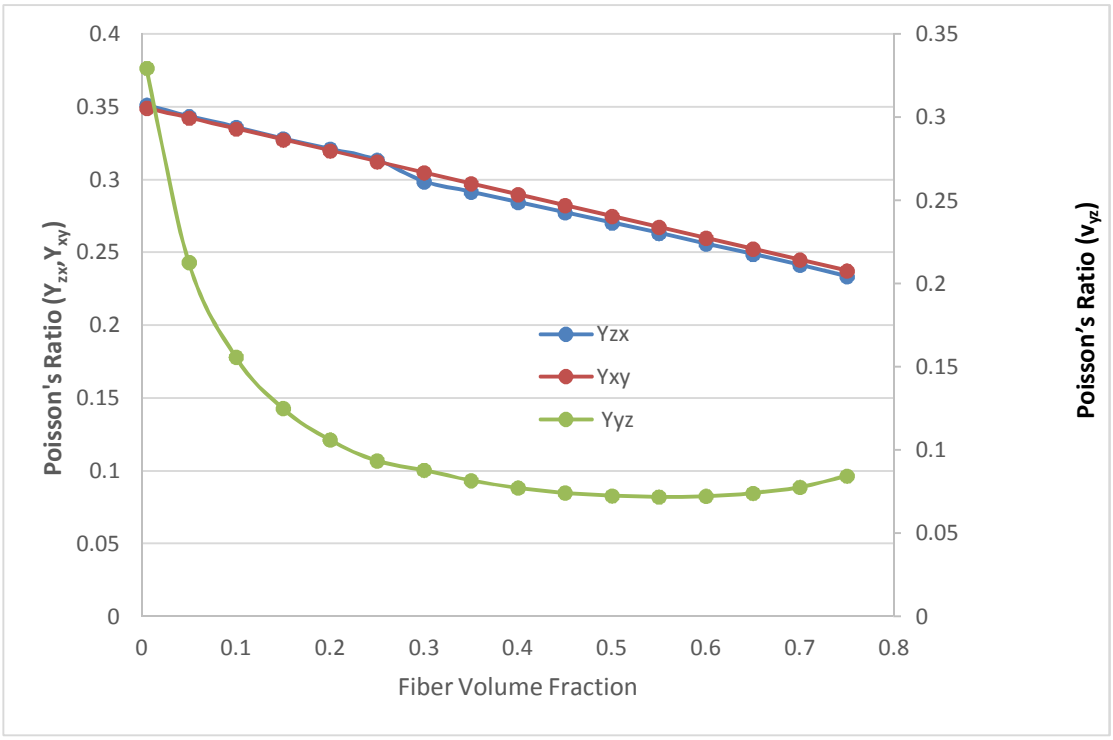

Figure 20: Material properties of the RVEs of Glass Fiber/Epoxy extracted from modeling. (a) Young's moduli, Ex and Ez, and shear moduli, Gxy and Gzx, and (b) Poisson's ratios vxy, vyz, and vzx.

5.5 Case Study-5:

Step 2: Characterize/Predict the performance of a 3D orthogonal polymeric matrix composite reinforced by microfibers

For the case study material a 3D orthogonal fabric composite of having 13 layers (seven layer fibers oriented in *x*-direction and six layer fibers oriented in *y*-direction) with binding of warp yarns through the thickness was selected. The thickness of each layer is 0.36 mm and the total thickness (*z*-direction) is 4.68 mm. Each period strips in *x*-direction (weft) and *y*-direction (warp) are 2.15mm and 2.55mm, respectively. This mutually perpendicular sets of yarns is a non-woven 3D fabric where carbon fiber reinforced with epoxy matrix composite. No interlacing (as with weaving), no interloping (as with knitting) or intertwining (as with braiding) of the involved yarns. This fabric architecture was described as "the action of producing a non-woven 3D-fabric by orientating orthogonally and binding the employed essentially three sets of yarns. The Non-interlacing is acronymed as noobing, Orientating Orthogonally and Binding, the main characteristics of the process and the fabric, which is called the noobed fabric. The fabric structure is also known under a variety of different other names. The most commonly used name is 3D orthogonal weave, but there are also other names for example: XYZ fabric, zero-crimp fabric, Cartesian fabric, DOS (directionally oriented structures) and polar fabric. [6]

To determine the properties under certain loading conditions the FEA model of the 3D model was developed. Along *x*-, *y*-, and *z*-directions uniaxial tensile tests were conducted, respectively, for extracting Young's moduli of E_x, E_y, and E_z, and Poisson's ratios of ν_{xy}, ν_{yx}, ν_{yz}, ν_{zy}, ν_{zx}, and ν_{xz}, respectively. In *x*-*y*, *y*-*z*, and *z*-*x* planes of the FEA model direct shear tests were also conducted, respectively, for extracting shear moduli of G_{xy}, G_{yz}, and G_{zx},

respectively. The elastic properties of the composite predicted by modeling are listed in Table.10. As carbon fiber volume fraction increases the In-plane (*x*-*y* plane) Young's moduli and shear moduli are linearly increases. Whereas, with carbon fiber volume fraction increases the Poisson's ratios decreases .The elastic properties of the case study composites by experiments were extracted by tensile tests and shear test. [8]

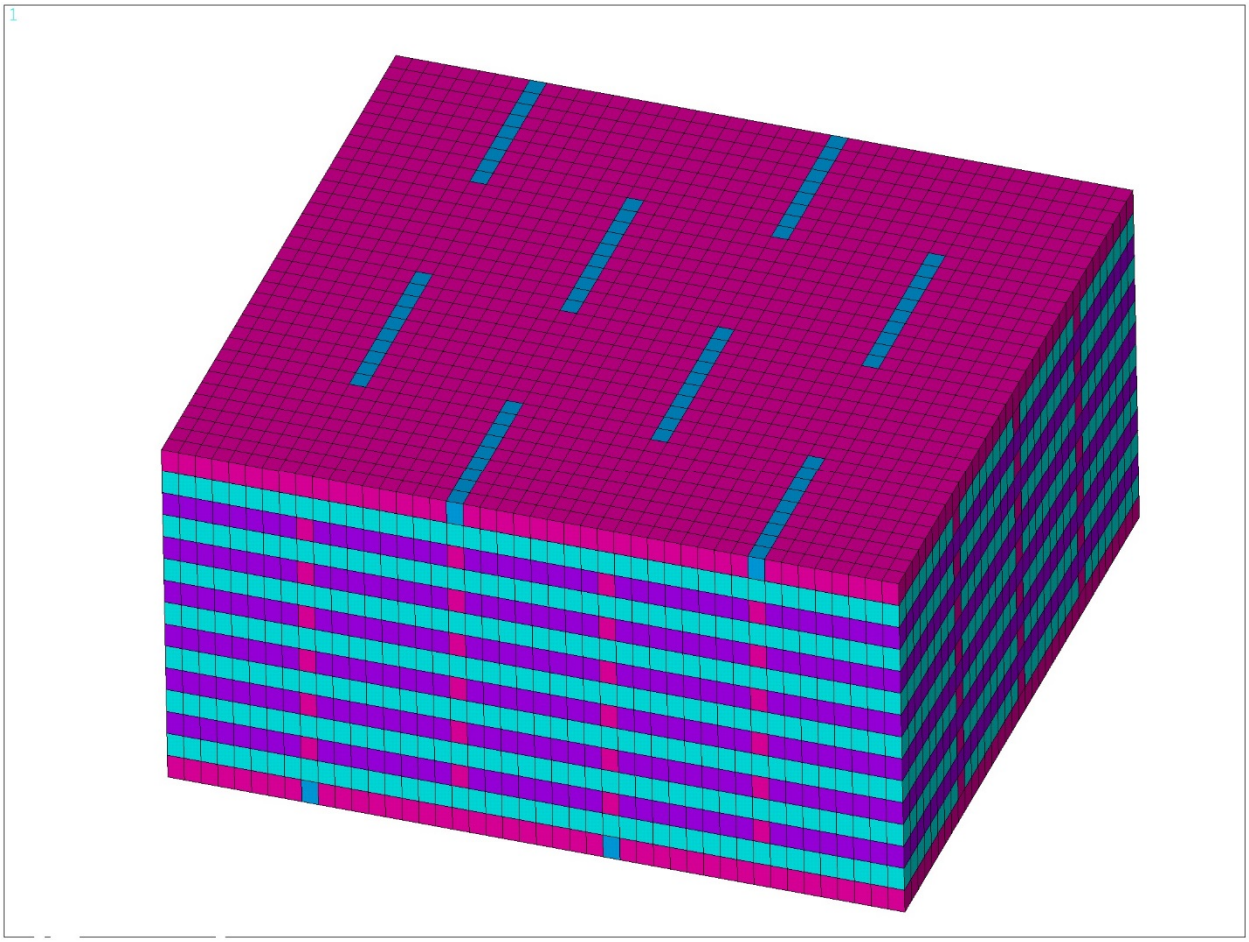

Figure 21: Finite Element Model of the 3-D orthogonal composite model.

Table 10: Material properties of the 3D orthogonal fabric composites from modeling (In-plane of x-y, 7 layers in x-direction, 6 layers in y-direction, and thickness of z-direction).

Fiber volume fraction V_f	**E_x (Gpa)**	**E_y (Gpa)**	**E_z (Gpa)**	**γ_{xy}**	**γ_{xz}**	**γ_{yx}**	**γ_{yz}**	**γ_{zx}**	**γ_{zy}**	**G_{xy} (Gpa)**	**G_{yz} (Gpa)**	**G_{zx} (Gpa)**
0.3	41.171	36.308	7.078	0.073	0.409	0.061	0.406	0.070	0.079	6.931	4.346	6.616
0.35	47.450	41.745	7.561	0.066	0.403	0.055	0.401	0.064	0.073	7.947	4.874	7.599
0.4	53.767	47.204	8.077	0.061	0.398	0.050	0.394	0.059	0.068	8.967	5.411	8.585
0.45	60.075	52.686	8.621	0.058	0.392	0.048	0.390	0.056	0.064	9.984	5.970	9.568
0.5	66.410	58.185	9.225	0.055	0.387	0.045	0.385	0.053	0.061	11.001	6.519	10.551
0.5265	**69.783**	**61.117**	**9.579**	**0.054**	**0.384**	**0.044**	**0.382**	**0.052**	**0.060**	**11.539**	**6.820**	**11.072**
0.55	72.776	63.720	9.896	0.053	0.382	0.043	0.380	0.051	0.059	12.017	7.100	11.533
0.6	79.178	69.293	10.633	0.051	0.377	0.042	0.375	0.050	0.058	13.035	7.687	12.517
0.65	85.626	74.920	11.481	0.050	0.372	0.041	0.371	0.049	0.057	14.052	8.272	13.500
0.7	92.140	80.623	12.467	0.050	0.368	0.041	0.367	0.049	0.057	15.069	8.909	14.483

Table 11: Comparison of material properties of the 3D orthogonal fabric case study composites (carbon fiber of 52.65 volume %) by modeling and experiments.

Fiber volume fraction, Vf= 56.25%	E_x (Gpa)	E_y (Gpa)	E_z (Gpa)	γ_{xy}	γ_{xz}	γ_{yx}	γ_{yz}	γ_{zx}	γ_{zy}	G_{xy} (Gpa)	G_{yz} (Gpa)	G_{zx} (Gpa)
Modeling	69.713	61.038	9.434	0.053	0.386	0.044	0.384	0.051	0.059	11.537	6.792	11.069
Experimental	67.330	64.260	___	0.075	___	___	___	___	___	12.040	___	___
% Difference	3.478	5.143		34.36						4.267		

(a)

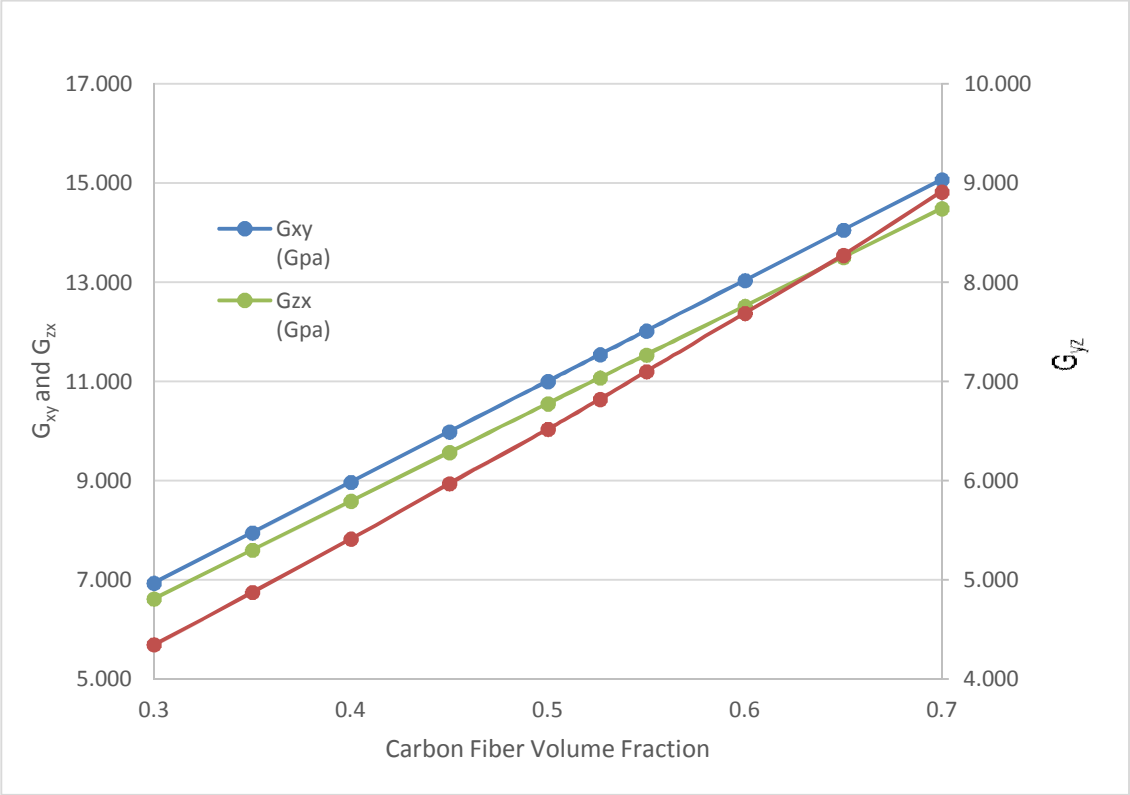
17.000
15.000
13.000
11.000
9.000
7.000
5.000
10.000
9.000
8.000
7.000
6.000
5.000
4.000
0.3
0.4
0.5
0.6
0.7
Gxy (Gpa)
Gzx (Gpa)
Gxy and Gzx
Gyz
Carbon Fiber Volume Fraction

(b)

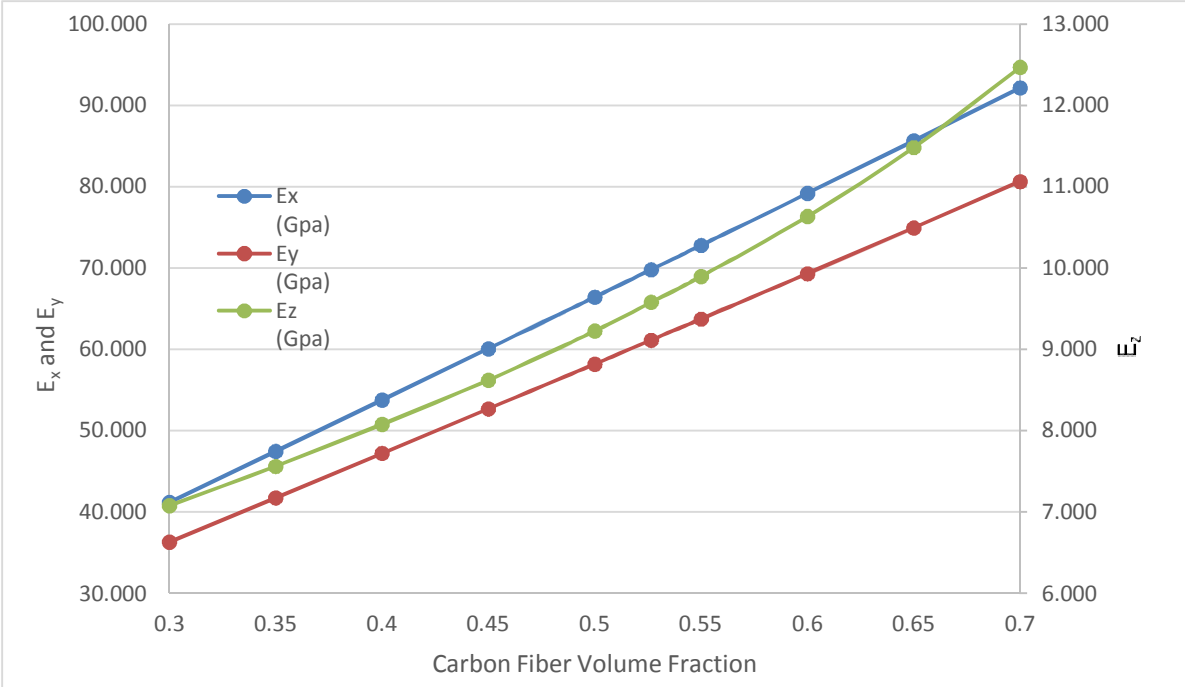
100.000
90.000
80.000
70.000
60.000
50.000
40.000
30.000
13.000
12.000
11.000
10.000
9.000
8.000
7.000
6.000
0.3
0.35
0.4
0.45
0.5
0.55
0.6
0.65
0.7
Ex (Gpa)
Ey (Gpa)
Ez (Gpa)
Ex and Ey
Ez
Carbon Fiber Volume Fraction

(c)

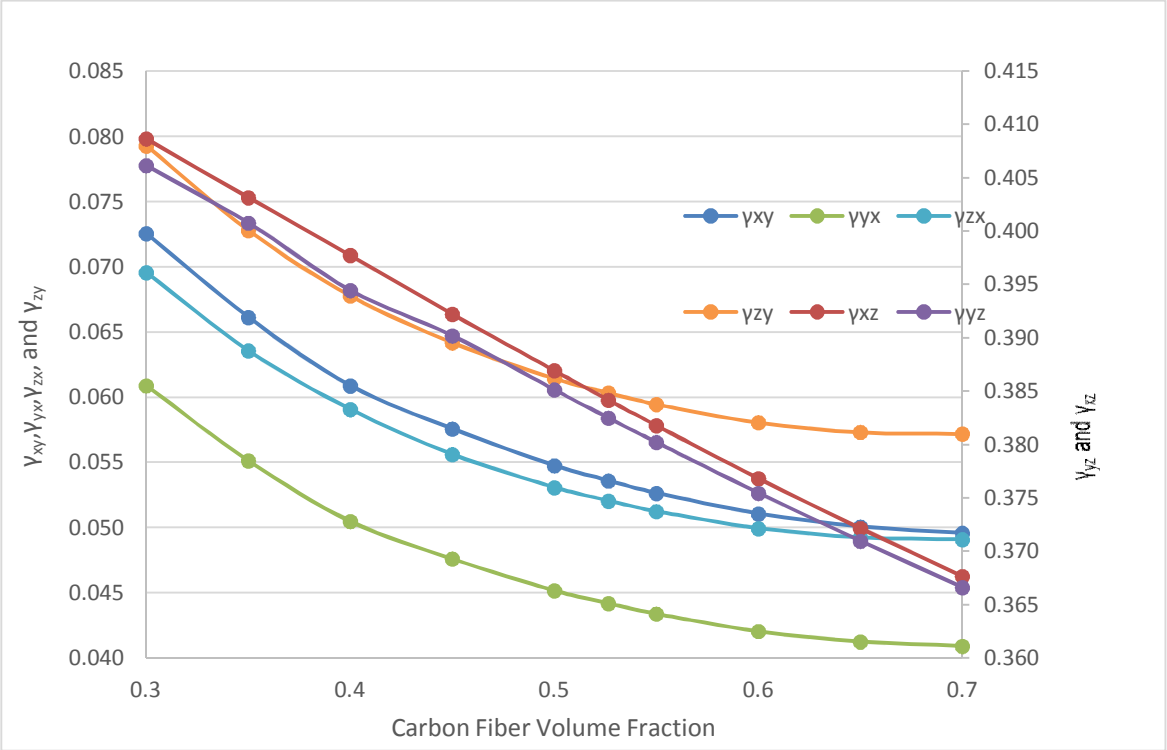

Figure 22: Elastic properties of the 3D orthogonal fabric composites changing with carbon fiber volume fraction. (a) Shear moduli, (b) Young's moduli, and(c) Poisson's ratios.

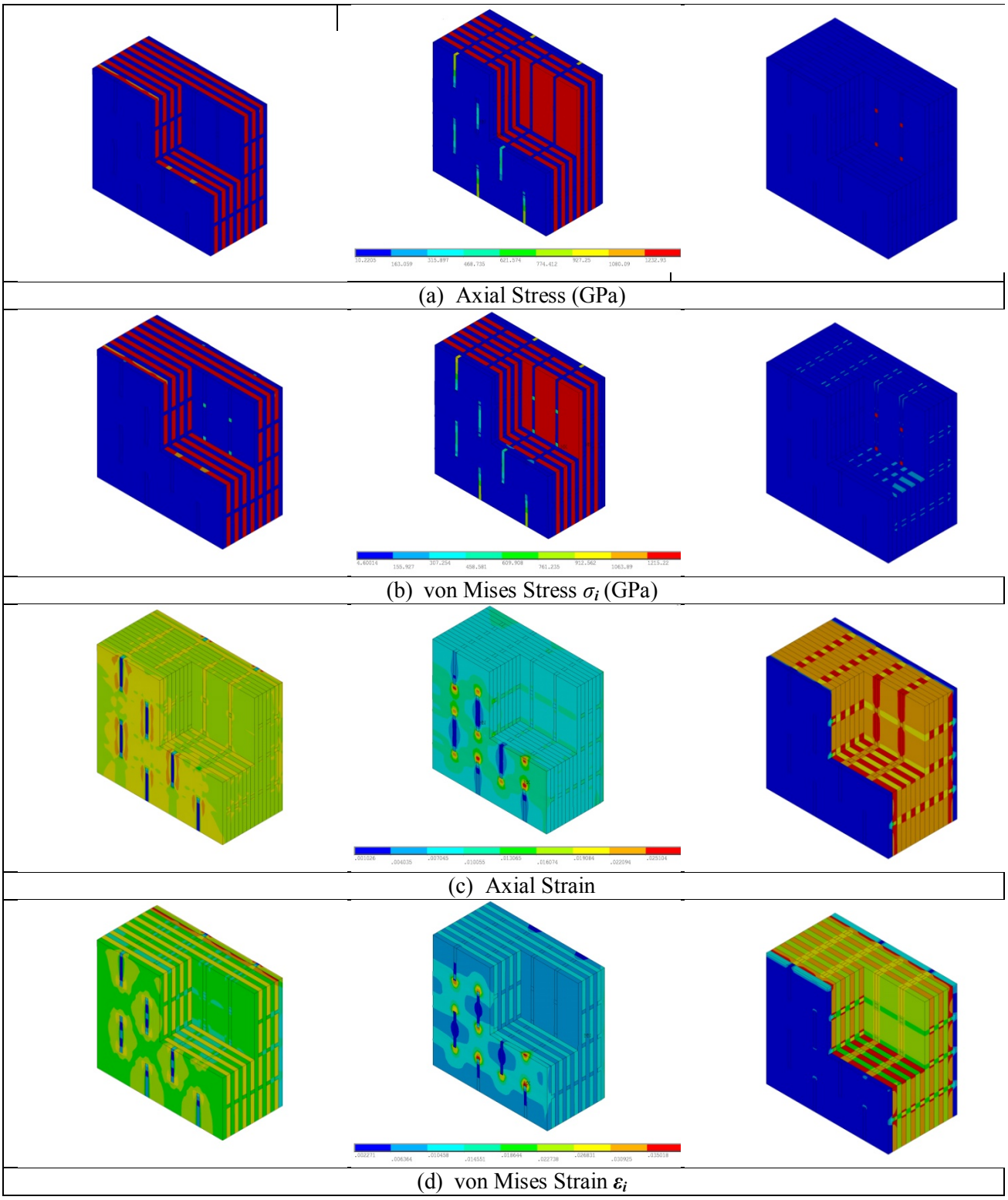

(a) Axial Stress (GPa)

(b) von Mises Stress σ_i (GPa)

(c) Axial Strain

(d) von Mises Strain ε_i

Figure 23:Tensile test for 3D orthogonal fabric CF/Epoxy composites at carbon fiber volume percent of 52.65 vol %.(left: tensile in x-component, middle: tensile in y-component, and right: tensile in z-component

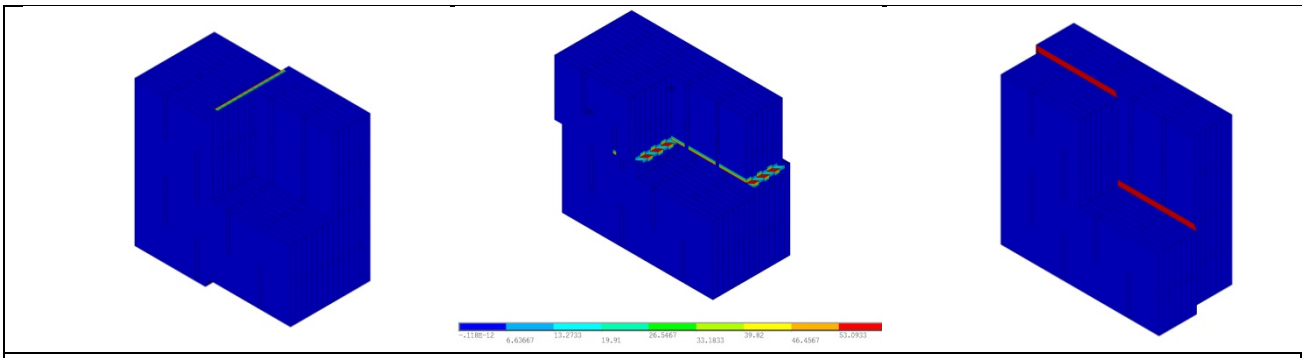

(a) Shear Stress (GPa)

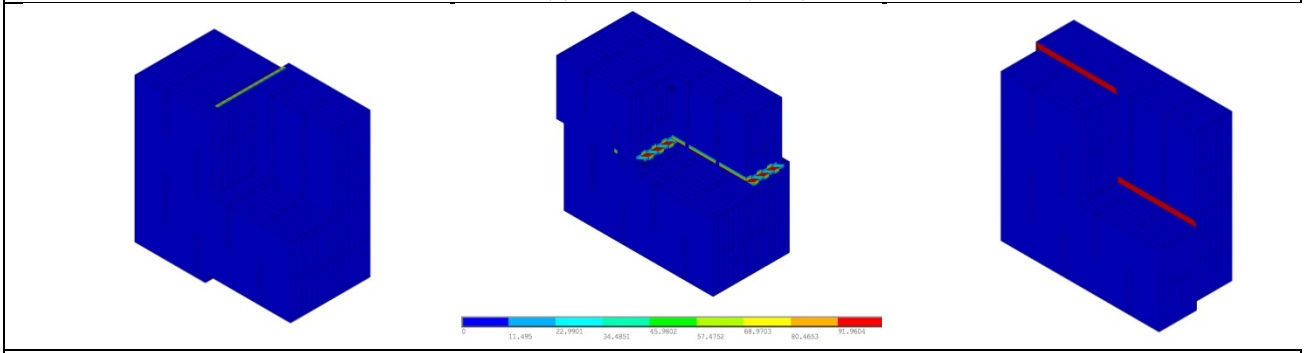

(b) von Mises Stress σ_i (GPa)

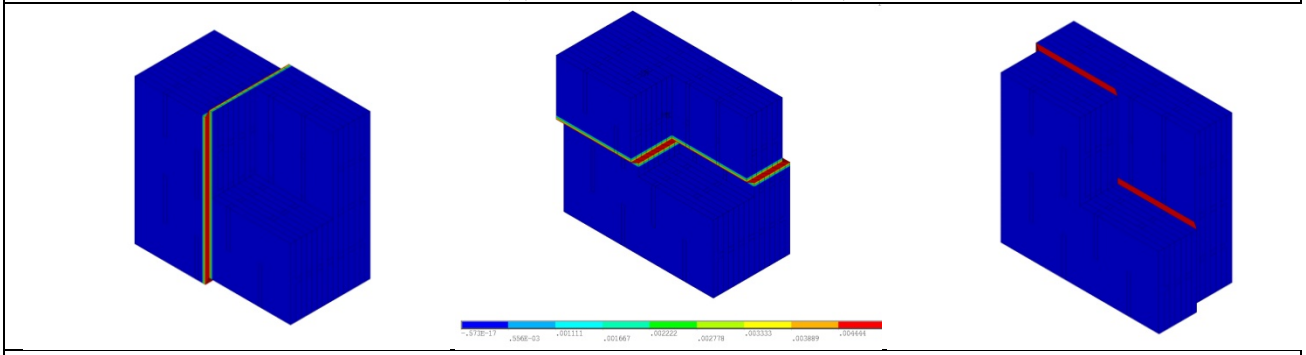

(c) Shear Strain

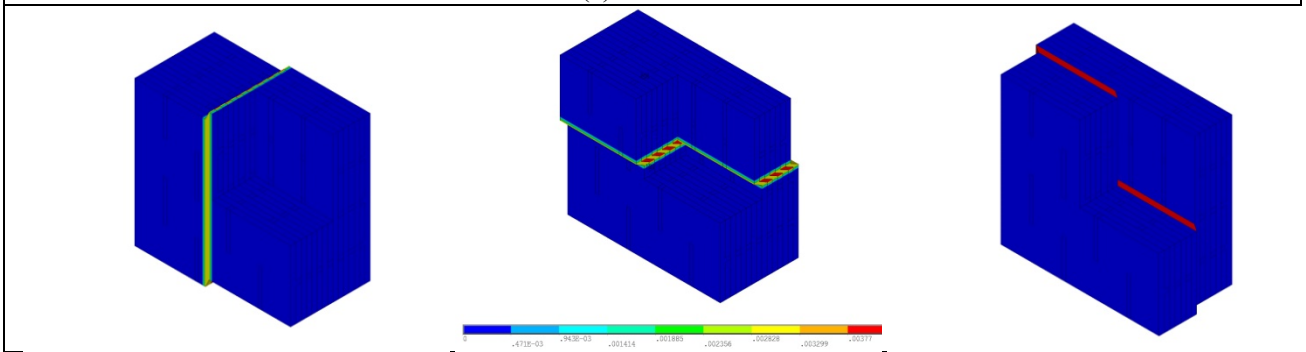

(d) von Mises Strain ε_i

Figure 24: Shear test for 3D orthogonal fabric CF/Epoxy composites at carbon fiber volume percent of 52.65 vol %.(left: tensile in xy-component, middle: tensile in yz-component, and right: tensile in zx-component)

5.6 Case Study-6:

Step 3: Characterize/Predict the performance of a 3D laminate polymeric matrix composite reinforced by microfibers

3-D Laminate Ply composite unit cell: Traditional laminated composites constitute the vast majority of applications, 3D orthogonal fabric composites have certain advantages over laminates because the amount of fiber in all three directions can be controlled, thereby enabling the designer to tailor the stiffness and strength of the final component to the exact specifications required for successful performance. 3D orthogonal fabric composites have superior through-the-thickness strength, stiffness, and thermal conductivity compared to conventional 2D laminated composites. Most of the published research on 3D orthogonal composites focuses on utilizing the experimental and predictive modeling techniques to evaluate the overall stiffness of the composite for various material designs. Some significant experimental and modeling results related to the process-induced residual stresses. But those papers are devoted to unidirectional laminates and do not cover the three-dimensional composite architectures. Therefore, the goal of this part is to develop realistic finite element models to predict 3D laminate ply composites and validate their predictions using micro-computed tomography (micro-CT) scans of actual samples.

A most common 3D laminate composite of having 13 layers (seven layer fibers oriented in x-direction and six layer fibers oriented in y-direction) without weaving warp yarns through the thickness was selected as the case study material. The thickness of each layer is 0.36 mm and the total thickness (z-direction) is 5.4 mm. Each period strips in x-direction (weft) and y-direction (warp) are 2.15mm and 2.55mm, respectively. This 3D

carbon fiber reinforced epoxy matrix composite is an orthogonal 3D composite laminate that essentially assembles two mutually perpendicular sets of yarns.

A finite element model of the 3D composite laminate model is developed for analysis using ANSYS education version software.

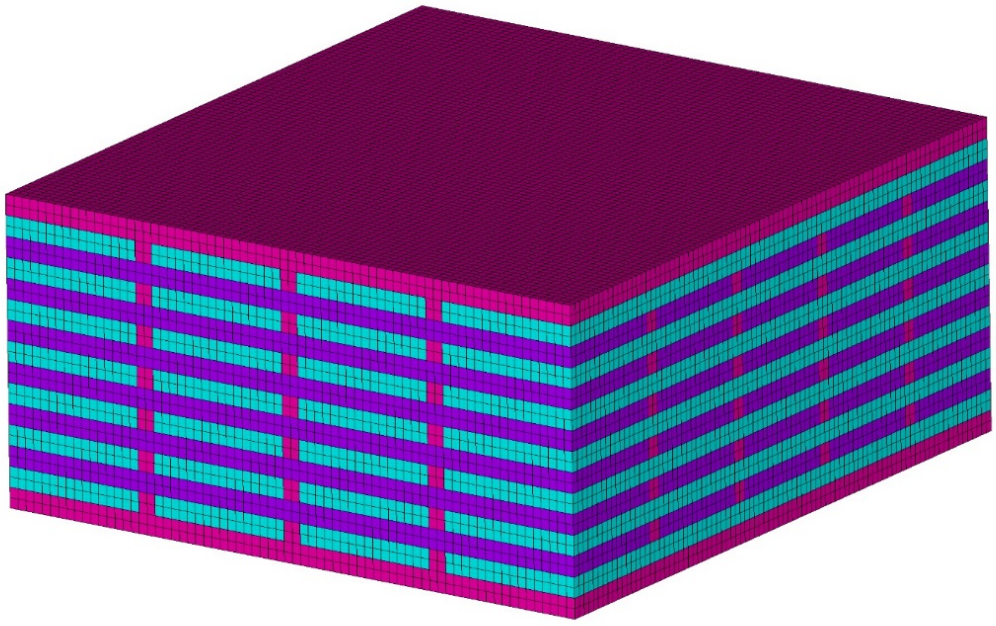

Figure 25: Finite Element Model of the 3-D laminate composite model.

Table 12: Material properties of the 3D orthogonal composite laminate from modeling (In-plane of x-y, 7 layers in x-direction, 6 layers in y-direction, and thickness of z-direction).

Fiber volume fraction V_f	**E_x (Gpa)**	**E_y (Gpa)**	**E_z (Gpa)**	**γ_{xy}**	**γ_{xz}**	**γ_{yx}**	**γ_{yz}**	**γ_{zx}**	**γ_{zy}**	**G_{xy} (Gpa)**	**G_{yz} (Gpa)**	**G_{zx} (Gpa)**
0.3	38.016	33.111	6.828	0.065	0.415	0.053	0.395	0.077	0.085	2.677	1.951	3.238
0.35	43.814	38.126	7.232	0.061	0.411	0.050	0.397	0.070	0.079	3.058	2.186	3.716
0.4	49.652	43.181	7.674	0.058	0.407	0.047	0.397	0.065	0.074	3.441	2.425	4.196
0.45	55.480	48.231	8.148	0.055	0.403	0.045	0.396	0.062	0.071	3.822	2.676	4.675
0.5	61.332	53.305	8.688	0.053	0.398	0.044	0.394	0.059	0.068	4.203	2.921	5.153

0.55	67.213	58.408	9.303	0.052	0.393	0.043	0.391	0.057	0.066	4.585	3.183	5.632
0.6	73.118	63.536	9.988	0.051	0.388	0.042	0.388	0.056	0.065	4.967	3.447	6.111
0.65	79.068	68.705	10.794	0.050	0.383	0.041	0.383	0.055	0.064	5.348	3.708	6.591
0.7	85.072	73.928	11.748	0.050	0.378	0.041	0.378	0.055	0.064	5.730	3.996	7.071

Table 13: Comparison of material properties of the 3D laminate case study composites (carbon fiber of 52.65 volume %) by modeling, experiments, and predicted customized model.

Fiber volume fraction, Vf= 56.25%	E_x (Gpa)	E_y (Gpa)	E_z (Gpa)	γ_{xy}	γ_{xz}	γ_{yx}	γ_{yz}	γ_{zx}	γ_{zy}	G_{xy} (Gpa)	G_{yz} (Gpa)	G_{zx} (Gpa)
Modeling with Z direction binding yarn	69.713	61.038	9.434	0.053	0.386	0.044	0.384	0.051	0.059	11.537	6.792	11.069
Experimental	67.330	64.260	___	0.075	___	___	___	___	___	12.040	___	___
Predicted Customized Model	63.76	56.60	8.90	0.052	0.396	0.43	0.393	0.067	0.066	4.356	3.056	5.347

a)

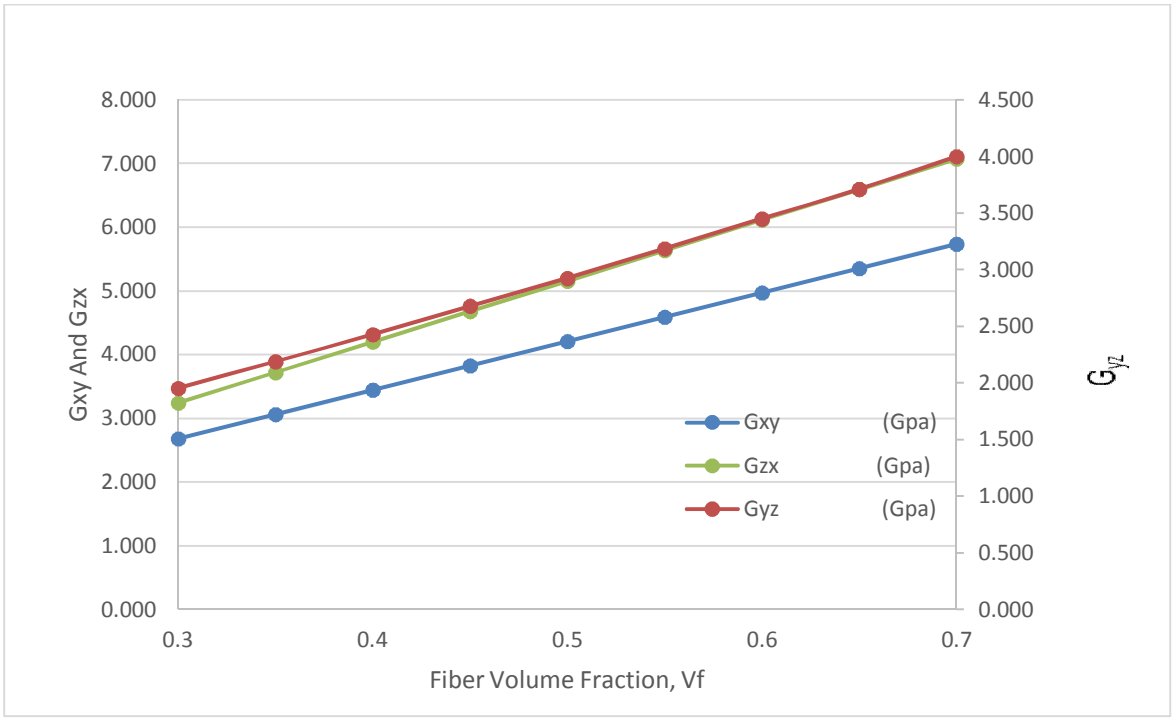

(b)

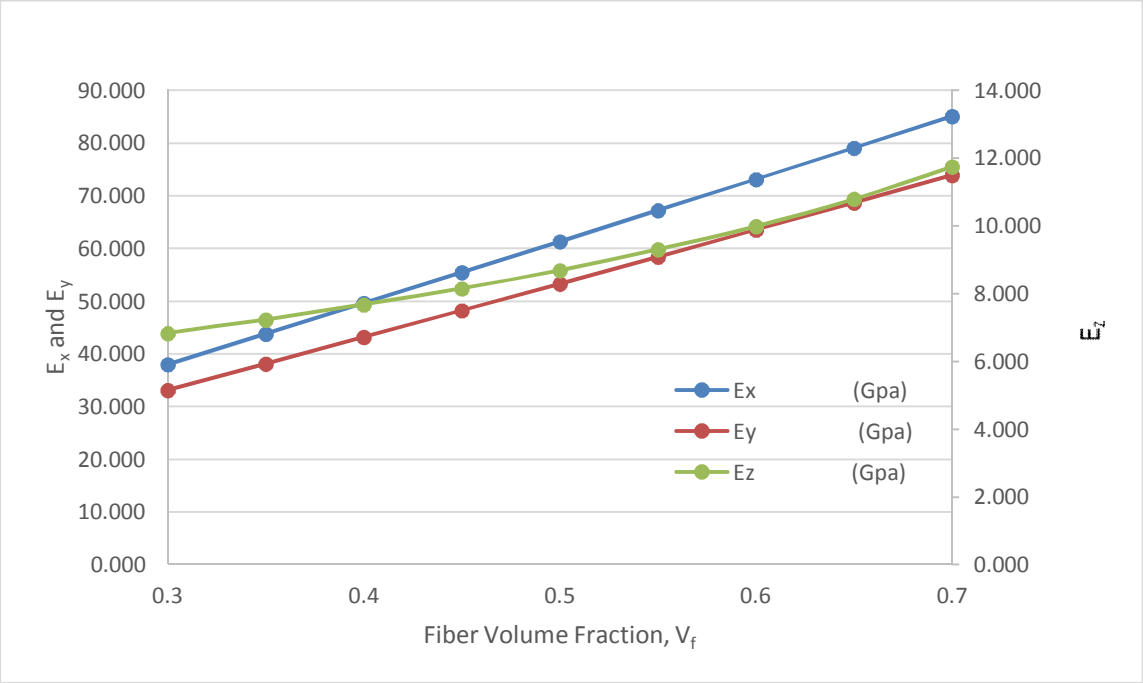

c)

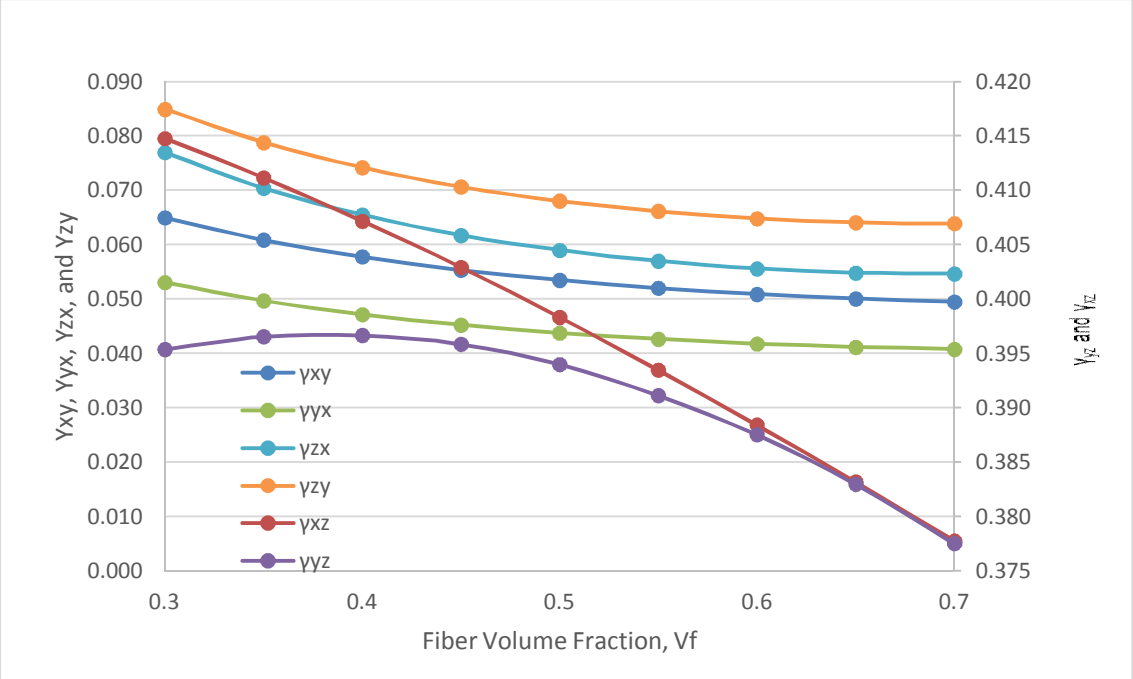

Figure 26: Elastic properties of the 3D orthogonal fabric composites changing with carbon fiber volume fraction. (a) Shear moduli, (b) Young's moduli, and(c) Poisson's ratios.

6. VALIDATION OF THE MODEL

According to the rule of mixtures the property of a composition can be calculated as the sum of its fundamental material properties multiplied by the corresponding volume fractions.

The equation of longitudinal young's modulus is derived as [24],

$$E_1 = E_f \upsilon_f + E_m \upsilon_m \text{---------- (E-1)}$$

6.1 First Order Model:

The first order model equation determines the longitudinal modulus of the ply. The equation of transverse young's modulus and in-plane shear modulus are derived as [24],

$$\frac{1}{E_2} = \frac{\nu_f}{E_f} + \frac{\nu_m}{E_m} - \frac{\nu_f \nu_m (E_f \gamma_m - E_m \gamma_f)^2}{E_f E_m (E_f \upsilon_f + E_m \upsilon_m)} \text{---------- (E-2)}$$

$$\frac{1}{G_{12}} = \frac{\upsilon_f}{G_f} + \frac{\upsilon_m}{G_m} \text{---------- (E-3)}$$

6.2 Second Order Model:

The second-order model of a ply provides better agreement with experimental results than the first-order model.

The derivation of the transverse young's modulus arrives at [24],

$$E_2 = \frac{\pi E_m r(\lambda)}{2\upsilon_f (1-\upsilon_m^2)} \text{---------- (E-4)}$$

On the other hand, the in-plane shear yields

$$G_{xy} = \frac{\pi G_m}{2\upsilon_f} r(\lambda) \text{---------- (E-5)}$$

Where,

$$\lambda = \frac{4v_f}{\pi} \text{---------- (E-6)}$$

$$r(\lambda) = \frac{1}{\sqrt{1-\lambda^2}} tan^{-1} \sqrt{\frac{1+\lambda}{1-\lambda}} - \frac{\pi}{4} \text{---------- (E-7)}$$

Glass Fiber-Epoxy Polymer composite:

The reference material properties of Glass fiber and Epoxy (from table.14) along the z-axis: fiber direction is taken for the validation purpose is as follows:

Table 14: Mechanical Properties of glass fiber and epoxy and z is the fiber direction.

Material	$E_x=E_y$ (GPa)	E_z (GPa)	$v_{xy}= v_{yx}$	$v_{zx} = v_{zy}$	$v_{xz} = v_{yz}$	G_{xy} (GPa)	G_{zx} (GPa)
Glass Fiber	86	86	0.2	0.2	0.2	35.8	35.8
Epoxy	3.5	3.5	0.35	0.35	0.35	1.29	1.29

Table 15: Longitudinal young's modulus characteristics of Glass Fiber/Epoxy calculated from FEA modeling and theoretical model (z-axis: fiber direction).

Fiber Volume Fraction Vf	From the FEA Model E1	Normalized longitudinal Young's Modulus from the FEA Model E1/Ef	From the equation,E-2 E1	Normalized Young's Modulus from the Rule of Mixture Model E1/Ef
	(GPa)		(GPa)	
0.005	3.89456	0.045285581	3.9125	0.045494186
0.05	7.55402	0.087837442	7.625	0.088662791
0.1	11.60744	0.134970233	11.75	0.136627907
0.15	15.75036	0.183143721	15.875	0.184593023
0.2	19.83306	0.230616977	20	0.23255814
0.25	23.97042	0.278725814	24.125	0.280523256
0.3	28.18792	0.327766512	28.25	0.328488372
0.35	32.30118	0.375595116	32.375	0.376453488
0.4	36.41424	0.423421395	36.5	0.424418605
0.45	40.52714	0.471245814	40.625	0.472383721
0.5	44.63946	0.519063488	44.75	0.520348837
0.55	48.75162	0.566879302	48.875	0.568313953
0.6	52.86338	0.614690465	53	0.61627907
0.65	56.9754	0.662504651	57.125	0.664244186
0.7	61.0871	0.710315116	61.25	0.712209302
0.75	65.19928	0.758131163	65.375	0.760174419

Table 16: Transverse young's modulus characteristics of Glass Fiber/Epoxy calculated from FEA modeling and theoretical model (z-axis: fiber direction).

Fiber Volume Fraction Vf	From the FEA Model	Normalized Transverse Young's Modulus from the FEA Model	From the equation,E-4	Normalized Transverse Young's Modulus from the 1st order Model	Normalized Transverse Young's Modulus from the 2nd order Model
	E2	E2/Em	E2	E2/Em	E2/Em
	(GPa)		(GPa)		
0.005	3.653872287	1.04396351	3.5170934	1.004883829	1.153622909
0.05	4.682887504	1.337967858	3.687856202	1.053673201	1.200675228
0.1	5.388677096	1.539622028	3.901281086	1.114651739	1.267863023
0.15	6.007445752	1.716413072	4.138032573	1.182295021	1.344194691
0.2	6.56652633	1.87615038	4.400995349	1.257427243	1.431431365
0.25	7.165447298	2.047270657	4.694659353	1.341331244	1.532151796
0.3	8.309186207	2.312245	5.02498465	1.4357099	1.649916059
0.35	9.062553875	2.589301107	5.399762534	1.542789296	1.789736643
0.4	9.906199758	2.830342788	5.829269917	1.665505691	1.958910042
0.45	10.87007278	3.10573508	6.327294139	1.807798325	2.16852558
0.5	11.99326225	3.426646359	6.912739795	1.975068513	2.43639722
0.55	13.32710183	3.807743381	7.612221564	2.174920447	2.793317596
0.6	14.9489934	4.271140972	8.464419331	2.418405523	3.298211773
0.65	16.99423017	4.855494335	9.527766325	2.72221895	4.082323771
0.7	19.70434306	5.629812303	10.89487822	3.112822349	5.523427866
0.75	23.69123709	6.768924882	12.72179711	3.634799174	10.06872999

Table 17: In-plane Shear modulus characteristics of Glass Fiber/Epoxy calculated from FEA modeling and theoretical model (z-axis: fiber direction).

Fiber Volume Fraction	From the FEA Model	Normalized Shear Modulus from the FEA Model	From the equation,E-3	Normalized Shear Modulus from the 1st order Model	Normalized Shear Modulus from the 2nd Order Model
Vf	G12 (GPa)	G12/Gm	G12	G12/Gm	G12/Gm
			(GPa)		
0.005	1.354038276	1.049642074	1.296247915	1.004843345	1.012304102
0.05	1.74409218	1.352009442	1.355326749	1.050640891	1.053592513
0.1	2.018231122	1.56452025	1.427622842	1.106684374	1.112549803
0.15	2.262691432	1.754024366	1.508066402	1.169043722	1.179530842
0.2	2.487320579	1.928155488	1.598116947	1.238850347	1.256081023
0.25	2.729694209	2.116042022	1.699604743	1.317523057	1.344463201
0.3	3.183596248	2.467904068	1.8148565	1.406865504	1.447801341
0.35	3.492313632	2.70721987	1.946875943	1.509206158	1.570493905
0.4	3.839612309	2.976443651	2.099609375	1.627604167	1.718943562
0.45	4.325112016	3.352800013	2.278346874	1.766160367	1.902881196
0.5	4.7032401	3.645922558	2.49034749	1.930501931	2.137938561
0.55	5.374652752	4.166397482	2.745849298	2.128565347	2.451136191
0.6	6.071813709	4.706832333	3.059772296	2.371916509	2.894180831
0.65	6.784123821	5.259010714	3.454740225	2.678093198	3.582239109
0.7	7.913390787	6.134411463	3.966789668	3.07503075	4.846807952
0.75	9.572217004	7.420323259	4.657039711	3.610108303	8.378302364

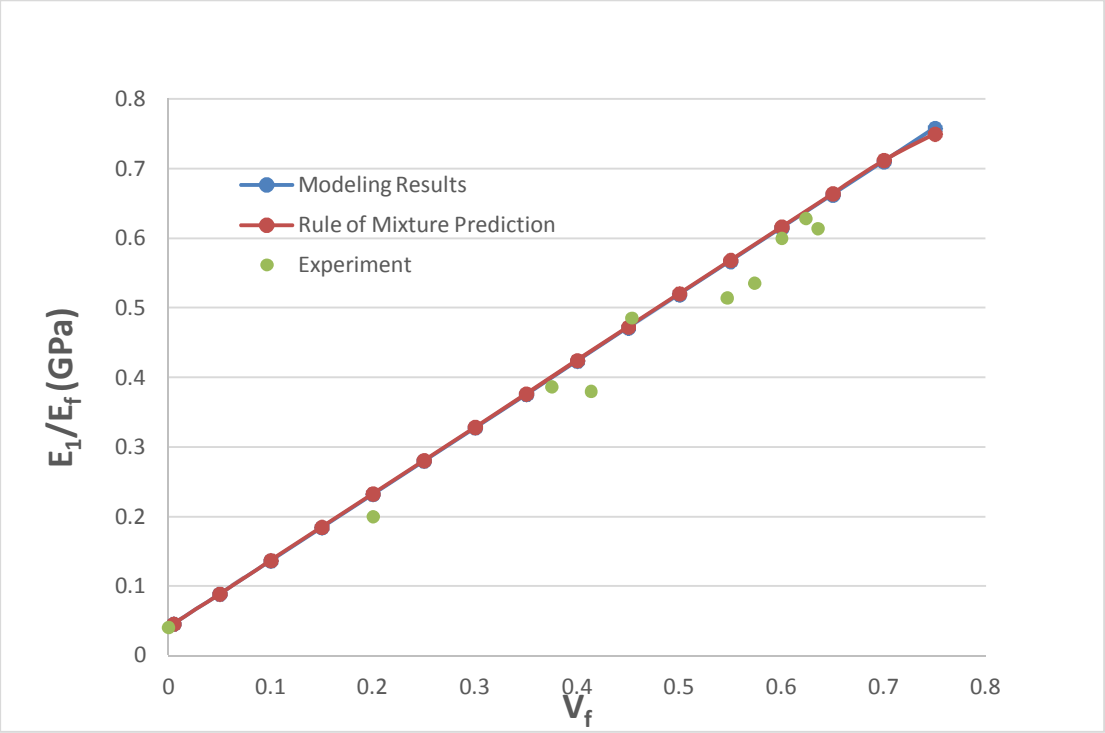

Figure 27: Longitudinal young's modulus characteristics of Glass Fiber/Epoxy calculated from FEA modeling, theoretical rule of mixture model, and Experiment (22).

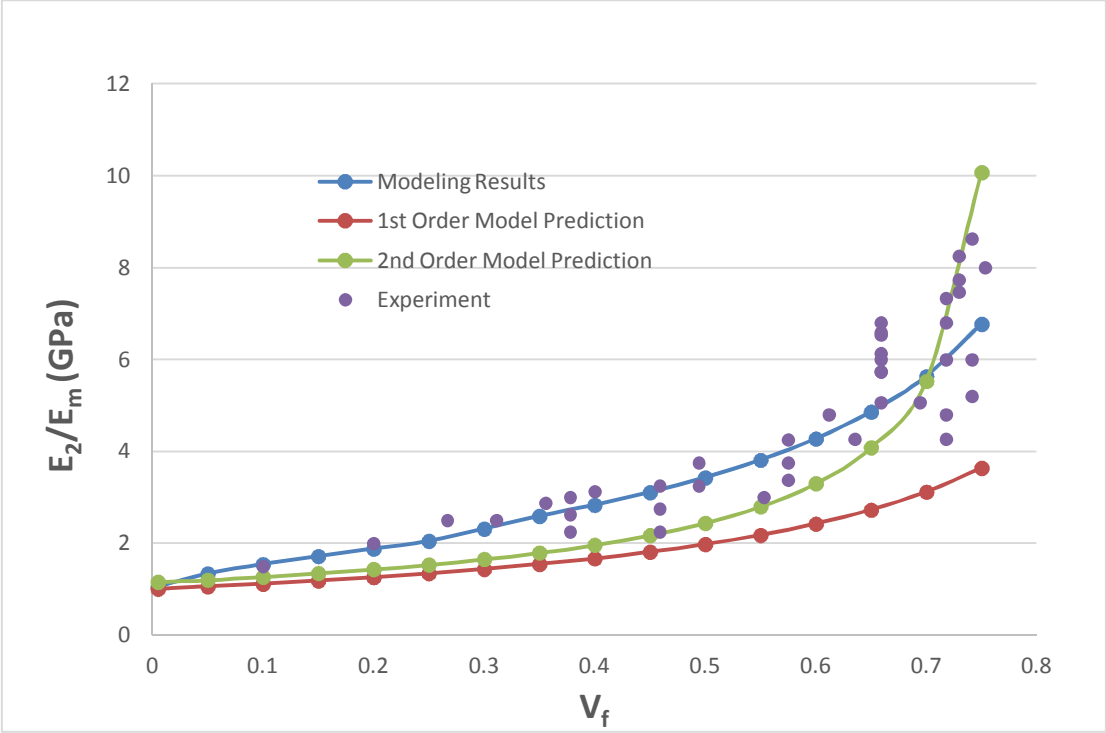

Figure 28: Transverse young's modulus characteristics of Glass Fiber/Epoxy composite materials calculated from FEA modeling, theoretical 1st order model, theoretical 2nd order model, and Experiment (21, 23).

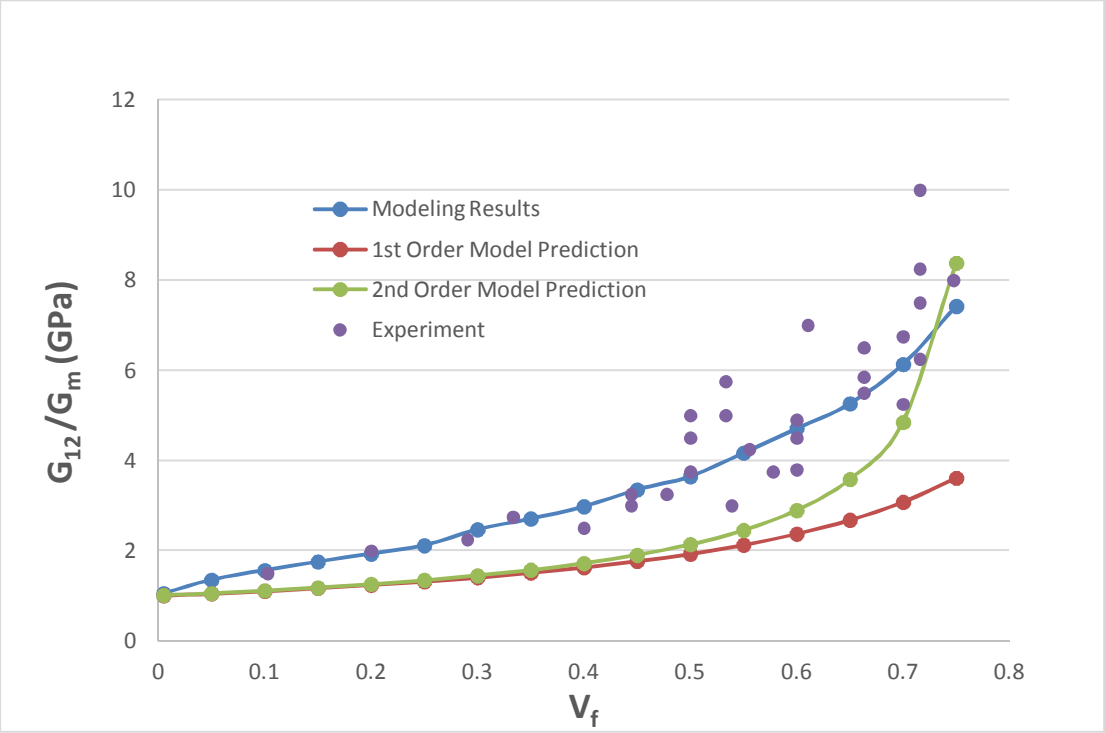

Figure 29: In-plane shear modulus characteristics of Glass Fiber/Epoxy calculated from FEA modeling, theoretical 1st order model, theoretical 2nd order model, and Experiment (22).

7. CONCLUSION

The modeling approach for five different case studies has effectively predicted the mechanical properties of IM7/PEEK, carbon fiber reinforced epoxy polymer composite, glass fiber reinforced epoxy, and carbon fiber reinforced polyamide 6. In step one, the micro-hetero structures of the composites were represented by 3D micro scale square and hexagonal RVE with a continuous carbon fiber in the matrix, taking into account of transversely isotropic properties of the carbon fibers. The mechanical properties of each RVE were extracted from the modeling results of the RVEs undergone three load tests, i.e., uniaxial tensile test, lateral expansion test, and transverse shear test, using the appropriate derived formulae. From the generated graph, we observed that the resultant values of Young's moduli and poison's ratios seem to be quite consistent based on their initial property values. The equivalent mechanical properties of the micro-hetero structures were obtained by averaging the mechanical properties extracted from each RVE. We also analyzed the glass fiber/epoxy composite from the FEA model along with theoretical values and experimental data. From the characteristics graph, we have seen that the finite element model of the composite shows agreement with the experimental data. In the validation part, the 3D orthotropic composite model was validated by comparing with the experimental available data. Computational modeling results for IM7-PEEK, Carbon Fiber-Epoxy, and Glass Fiber-Epoxy composites are analyzed and validated based on mathematical equations and experimental results.

After evaluating the mechanical properties of the micro-heterostructure a comparative analysis is performed based on previous research works. Finite element model of the

unit cell of a 3-D orthogonal composite structure is characterized based on the experimental data at 52.65% and showed reasonably accurate and thus validated. Finite element model of the unit cell of a 3-D Laminate composite structure is predicted based on the above analytical studies.

8. FUTURE WORKS

- An analysis on 3-D woven composites reinforced by carbon continuous fiber along with the representative volume element of the plain weave geometry can be conducted for each step to validate the mathematical model and derivation of the properties from the reference journal resources.
- An experimental analysis on and the laminated ply finite element model can be performed to validate the computational model.
- From the randomly oriented carbon short fiber with variable length size will be considered to predict the properties of different sets of composite materials. Eventually,
- The properties of the other formats of multi-scale polymeric composites reinforced by micro/nano-fibers can be characterized/predicted.

REFERENCES

1. "Composites", Last modified on November 21,2011,http://www.slideshare.net/BUKMAS/composites-10363428
2. "Composite Materials ", Last modified on March18,2014, http://www.slideshare.net/MohsinAli70/composite-presentation-32469042
3. "Discontinuous Fiber Types", Last modified on December 16,2013, https://www.google.com/search?q=fabrication+process+of+composite+materials&biw=1600&bih=805&source=lnms&tbm=isch&sa=X&sqi=2&ved=0ahUKEwjPjoXO0P3LAhWKmoMKHa9cDdcQ_AUIBigB#tbm=isch&q=Spray+Molding+fabrication+process&imgrc=cg8lAI8MrGp1aM%3A
4. "UG PMC Processing", Last modified on April 30,2012, https://www.google.com/search?q=fabrication+process+of+composite+materials&biw=1600&bih=805&source=lnms&tbm=isch&sa=X&sqi=2&ved=0ahUKEwjPjoXO0P3LAhWKmoMKHa9cDdcQ_AUIBigB#tbm=isch&q=pultrusion+fabrication+process&imgrc=F6lVQtEBNF2mtM%3A
5. "Properties of Fiber Composites", Copyright 2012, https://www.google.com/search?q=polymer+matrix+composite+fabrication+process&espv=2&biw=1366&bih=667&source=lnms&tbm=isch&sa=X&ved=0ahUKEwjS2rey0v3LAhUGyYMKHW-YCbMQ_AUIBigB#tbm=isch&q=pultrusion&imgrc=sLFgdZ3pA_xP0M%3A
6. "UG PMC Processing", Last modified on April 30,2012, https://www.google.com/search?q=fabrication+process+of+composite+materials&biw=1600&bih=805&source=lnms&tbm=isch&sa=X&sqi=2&ved=0ahUKEwjPjoXO0P3LAhWKmoMKHa9cDdcQ_AUIBigB#tbm=isch&q=pultrusion+fabrication+process&imgrc=F6lVQtEBNF2mtM%3A
7. "Quality Assurance and Nondestructive Evaluation of Composite Materials", Last modified on April7,2015, https://www.google.com/search?q=fabrication+process+of+composite+materials&biw=1600&bih=805&source=lnms&tbm=isch&sa=X&sqi=2&ved=0ahUKEwjPjoXO0P3LAhWKmoMKHa9cDdcQ_AUIBigB#tbm=isch&q=Prepreg+fabrication+process&imgrc=zTKuYPKNi08bkM%3A
8. Hu, Zhong, and Ranjan Karki. "Prediction of mechanical properties of three-dimensional fabric

composites reinforced by transversely isotropic carbon fibers." Journal of Composite Materials (2014): 0021998314535960.

9. Banerjee, Sayan, and Bhavani V. Sankar. "Mechanical properties of hybrid composites using finite element method based micromechanics." *Composites Part B: Engineering* 58 (2014): 318-327.
10. Wang, Bai-Chen, Xia Zhou, and Ke-Ming Ma. "Fabrication and properties of CNTs/carbon fabric hybrid multiscale composites processed via resin transfer molding technique." *Composites Part B: Engineering* 46 (2013): 123-129.
11. Boroujeni, A. Y., M. Tehrani, A. J. Nelson, and M. Al-Haik. "Hybrid Carbon Nanotube-Carbon Fiber Composites with Improved In-plane Mechanical Properties." *Composites Part B: Engineering* (2014).
12. Zhang, Yongli, Yan Li, Hao Ma, and Tao Yu. "Tensile and interfacial properties of unidirectional flax/glass fiber reinforced hybrid composites." *Composites Science and Technology* 88 (2013): 172-177.
13. Lee, Doo Jin, Hwajin Oh, Young Seok Song, and Jae Ryoun Youn. "Analysis of effective elastic modulus for multiphased hybrid composites." *Composites Science and Technology* 72, no. 2 (2012): 278-283.
14. Fu, SY. Xu, G., and Mai, YW. "On the elastic modulus of hybrid particle/short-fiber/polymer composites" *DOI: 10.1016/S1359-8368(02)00013-6*
15. Venkateshwaran, N., A. Elayaperumal, and G. K. Sathiya. "Prediction of tensile properties of hybrid-natural fiber composites." *Composites Part B: Engineering* 43, no. 2 (2012): 793-796.
16. George, T., V. S. Deshpande, and H. N. G. Wadley. "Hybrid Carbon Fiber Composite Lattice Truss Structures." *Composites Part A: Applied Science and Manufacturing* (2014).
17. Mishnaevsky Jr, L., and Dai, G." Hybrid and hierarchical nanoreinforced polymer composites: Computational modelling of structure–properties relationships*" DOI: 10.1016/j.compstruct.2014.06.027.*
18. Muñoz, R., V. Martínez, F. Sket, C. González, and J. LLorca. "Mechanical behavior and failure micromechanisms of hybrid 3D woven composites in tension." *Composites Part A: Applied Science and Manufacturing* 59 (2014): 93-104.

19. Rahmanian, S., A. R. Suraya, M. A. Shazed, R. Zahari, and E. S. Zainudin. "Mechanical characterization of epoxy composite with multiscale reinforcements: Carbon nanotubes and short carbon fibers." *Materials & Design* 60 (2014): 34-40.
20. Chen, Qi, Lifeng Zhang, Yong Zhao, Xiang-Fa Wu, and Hao Fong. "Hybrid multi-scale composites developed from glass microfiber fabrics and nano-epoxy resins containing electrospun glass nanofibers." *Composites Part B: Engineering* 43 (2) (2012): 309-316.
21. Tarnopol'skii, Yu.M. and Roze, A.V. (1969). Specific Features of Analysis for Structural Elements of Reinforced Plastics. Riga, Zinatne (in Russian).
22. Lee, D.J., Jeong, T.H. and Kim, H.G. (1995). Effective longitudinal shear modulus of unidirectional composites. In Proc. 10 th Int. Conf. on Composite Materials (ICCM-IO), Vo1.4, Characterization and Ceramic Matrix Composites, Canada, 1995, pp. 171-1 78.
23. Kondo, K. and Aoki, T. (1982). Longitudinal shear modulus of unidirectional composites. In *Proc. 4th Int. Conference on Composite Materials (ICCM-IV), Vol.1, Program in Science and Engineering of Composites* (Hayashi, Kawata and Umeka eds.). Tokyo, 1982, pp. 357-364.
24. Valery V. Vasiliev and Evgeny V. Morozov, Preface to the Third Edition, In Advanced Mechanics of Composite Materials (Third Edition), Elsevier, Boston, 2013, Pages xi-xiii, ISBN 9780080982311, http://dx.doi.org/10.1016/B978-0-08-098231-1.05001-9.

(http://www.sciencedirect.com/science/article/pii/B9780080982311105001)